Molecular Biology of the Cell
Vol. 7, 769-789, May 1996

Different Subcellular Localization of *Saccharomyces cerevisiae* HMG-CoA Reductase Isozymes at Elevated Levels Corresponds to Distinct Endoplasmic Reticulum Membrane Proliferations

Ann J. Koning, Christopher J. Roberts, and Robin L. Wright*

Department of Zoology, University of Washington, Seattle, Washington 98195

Submitted September 8, 1995; Accepted February 21, 1996
Monitoring Editor: Randy W. Schekman

In all eucaryotic cell types analyzed, proliferations of the endoplasmic reticulum (ER) can be induced by increasing the levels of certain integral ER proteins. One of the best characterized of these proteins is HMG-CoA reductase, which catalyzes the rate-limiting step in sterol biosynthesis. We have investigated the subcellular distributions of the two HMG-CoA reductase isozymes in *Saccharomyces cerevisiae* and the types of ER proliferations that arise in response to elevated levels of each isozyme. At endogenous expression levels, Hmg1p and Hmg2p were both primarily localized in the nuclear envelope. However, at increased levels, the isozymes displayed distinct subcellular localization patterns in which each isozyme was predominantly localized in a different region of the ER. Specifically, increased levels of Hmg1p were concentrated in the nuclear envelope, whereas increased levels of Hmg2p were concentrated in the peripheral ER. In addition, an Hmg2p chimeric protein containing a 77-amino acid lumenal segment from Hmg1p was localized in a pattern that resembled that of Hmg1p when expressed at increased levels. Reflecting their different subcellular distributions, elevated levels of Hmg1p and Hmg2p induced sets of ER membrane proliferations with distinct morphologies. The ER membrane protein, Sec61p, was localized in the membranes induced by both Hmg1p and Hmg2p green fluorescent protein (GFP) fusions. In contrast, the lumenal ER protein, Kar2p, was present in Hmg1p:GFP membranes, but only rarely in Hmg2p:GFP membranes. These results indicated that the membranes synthesized in response to Hmg1p and Hmg2p were derived from the ER, but that the membranes were not identical in protein composition. We determined that the different types of ER proliferations were not simply due to quantitative differences in protein amounts or to the different half-lives of the two isozymes. It is possible that the specific distributions of the two yeast HMG-CoA reductase isozymes and their corresponding membrane proliferations may reveal regions of the ER that are specialized for certain branches of the sterol biosynthetic pathway.

INTRODUCTION

The endoplasmic reticulum (ER)[1] is a dynamic organelle necessary for protein secretion and lipid biosynthesis in eukaryotes. Although the membranes that comprise the ER are physically contiguous, the ER consists of multiple subdomains (for review see Sitia and Meldolesi, 1992; Vertel *et al.*, 1992). Originally distinguished by morphological differences, these subdomains include the smooth ER, rough ER, the transitional ER, and the nuclear envelope (Palade, 1975; Fawcett, 1981; Rose and Doms, 1988). Although certain proteins, including the ER chaperone, BiP, and protein disulfide isomerase, appear to be distributed throughout the entire ER (Sitia and Meldolesi, 1992),

* Corresponding author.
[1] Abbreviations used: ER, endoplasmic reticulum; HMG, 3-hydroxy 3-methylglutaryl coenzyme A; HMGR, 3-hydroxy 3-methylglutaryl coenzyme A reductase; DiOC6, 3,3'-dihexyloxacarbocyanineiodide; BiP, binding protein.

other proteins are limited to specific ER regions. For example, epoxide hydrolase is a classical marker of smooth ER (Galteau *et al.*, 1985), and the lamin B receptor is localized in the inner nuclear envelope (Smith and Blobel, 1993). Proteins involved in calcium storage and release are also found in specialized regions of the ER. For example, the Ca^{++} binding protein, calsequestrin, is localized in smooth ER regions and concentrated in vesicles in Purkinje neurons (Villa *et al.*, 1991; Takei *et al.*, 1992), but is present only in the terminal cisternae of the sarcoplasmic reticulum in skeletal muscle (Franzini-Armstrong *et al.*, 1987). In addition, the inositol 1,4,5-trisphosphate receptor, a Ca^{++} channel, is concentrated in cisternal ER stacks in Purkinje neurons (Satoh *et al.*, 1990; Takei *et al.*, 1992). These proteins provide biochemical markers that can be correlated with morphology to distinguish specialized regions of the ER.

In the yeast *Saccharomyces cerevisiae*, the ER consists of the nuclear envelope connected to a network of peripheral ER tubules that underlie the plasma membrane (Matile *et al.*, 1969; Preuss *et al.*, 1991). Many proteins are localized throughout the ER in yeast, including the yeast homologue of BiP, Kar2p (Rose *et al.*, 1989), proteins involved in translocation, such as Sec62p (Deshaies and Schekman, 1990) and Sec63p (Feldheim *et al.*, 1992), enzymes involved in protein modification, including dolichol-phosphate-mannose-synthase (Preuss *et al.*, 1991), and the protein disulfide isomerase homologue, Eug1p (Tachibana and Stevens, 1992), as well as a protein thought to be involved in vacuolar ATPase assembly in the ER, Vma21p (Hill and Stevens, 1994). Beyond the morphological distinction between the nuclear envelope and the peripheral ER, specialized subdomains of the yeast ER are not evident from the localization patterns of these various proteins. However, several examples exist that suggest specialized ER subdomains are present in yeast. For instance, certain areas of the yeast ER accumulate Kar2p in "BiP bodies" when ER to Golgi traffic is arrested (Nishikawa *et al.*, 1994). The authors suggest in one model that a block in ER to Golgi traffic may cause BiP to accumulate in an ER subdomain that defines the site of protein export (Nishikawa *et al.*, 1994). In addition, a specific sub-fraction of the ER is associated with the mitochondria (Gaigg *et al.*, 1995). Finally, another example of ER specialization comes from analysis of HMG-CoA (3-hydroxy-3-methylglutaryl coenzyme A) reductase, a protein that can trigger an alteration of a specific region of the ER (Wright *et al.*, 1988).

HMG-CoA reductase (HMGR) is an integral ER protein that catalyzes the rate-limiting step in the sterol biosynthetic pathway. In addition to sterols, this pathway also provides the cell with nonsterol metabolites, including isopentyl-adenine, dolichols, ubiquinone, and prenyl groups for use in protein translation, glycosylation, electron transport, and protein modification. In mammalian cells, the amount of HMGR is tightly regulated at multiple levels, including transcription, translation, and post-translation (see review by Goldstein and Brown, 1990). For example, the degradation of HMGR is modulated in response to the availability of both sterols and nonsterol metabolites (Roitelman and Simoni, 1992).

All animals that have been examined contain a single HMGR gene. In contrast, *S. cerevisiae* contains two genes, *HMG1* and *HMG2*, that both encode functional HMGR isozymes. These genes are estimated to have arisen from a duplication event that occurred approximately 56 million years ago (Lum, Edwards, and Wright, unpublished results). Interestingly, although the catalytic function of the two isozymes is identical, expression of the two yeast isozymes is regulated differently. *HMG1* transcription is highest in the presence of oxygen, and this regulation is mediated through the heme-binding protein Hap1p (Thorsness *et al.*, 1989). When either oxygen or heme levels are depleted, transcription of *HMG1* decreases 10-fold. In contrast, when oxygen or heme is depleted, transcription of *HMG2* increases threefold. In addition to differences in transcription, *HMG1* and *HMG2* encode proteins that have different stabilities. Hmg2p has a short half-life of about 50-60 min, whereas Hmg1p has a half-life greater than 4 h (Hampton and Rine, 1994). As in mammalian cells, the degradation of Hmg2p is regulated by a nonsterol metabolite of the mevalonate pathway such that when flux through the pathway is low, Hmg2p stability increases (Hampton and Rine, 1994).

The predicted topologies of yeast and mammalian HMGR are similar. Both possess a cytosolic catalytic domain and a complex amino-terminal domain that passes through the ER membrane seven or eight times. The amino acid sequence of the HMGR catalytic domain is highly conserved, with 65% amino acid identity between the catalytic domains of mammalian and yeast HMGRs, and 95% amino acid identity between the two yeast catalytic domains (Basson *et al.*, 1988). In contrast, there is no observable amino acid conservation between the membrane domains of yeast and mammalian HMGRs. However, the membrane domains of the two yeast HMGRs are 46% identical (Basson *et al.*, 1988). The function of the membrane domain includes mediating the regulated degradation of both the mammalian and yeast HMGRs (Gil *et al.*, 1985; Skalnik *et al.*, 1988; Hampton and Rine, 1994) and the proliferation of ER membranes when HMGR levels increase (Jingami *et al.*, 1987; Parrish *et al.*, 1995).

Both yeast Hmg1p and mammalian HMGRs trigger the proliferation of cell-type–specific membranes

when expression levels are increased. In mammalian cells, HMGR induces the formation of crystalloid ER, which consists of hexagonal arrays of smooth ER tubules that arise from outfoldings of the nuclear envelope (Chin *et al.*, 1982; Pathak *et al.*, 1986). In yeast, Hmg1p triggers the formation of karmellae, which are stacked pairs of membranes associated with the nucleus (Wright *et al.*, 1988). Interestingly, the type of membrane proliferation induced depends on the cell-type (mammalian or yeast), rather than on the source of HMGR (Wright *et al.*, 1990). Specifically, increased levels of mammalian HMGR in yeast induce the formation of karmellae, not crystalloid ER, and increased levels of the Hmg1p in mammalian cells induce the proliferation of crystalloid ER, not karmellae. Therefore, it appears that cells respond to elevated levels of HMGR by proliferating a cell-type–specific membrane array. However, one observation involving the other HMGR isozyme, Hmg2p, suggested that this response may be more complicated.

Increased levels of Hmg2p infrequently triggered the formation of membrane stacks in the peripheral ER that were distinct from karmellae (Wright *et al.*, 1988). This result suggested the possibility that the two HMGR isozymes were localized differently in the ER. We have explored this possibility and found that increased levels of Hmg1p and Hmg2p were concentrated in different regions of the ER, and that each isozyme induced the proliferation of distinct sets of membrane arrays. However, the Hmg2p-induced membrane proliferations did not become abundant until later in the growth phase of yeast than that originally assayed by electron microscopy (Wright *et al.*, 1988). Thus, it is apparent that yeast can respond to two similar proteins in different ways. These results also suggest that the ER is not homogeneous in yeast, but that there are specialized ER regions, some of which may relate to the role the two HMGR isozymes have as key regulators of the sterol pathway.

MATERIALS AND METHODS

Yeast Strains and Growth Conditions

The yeast strains used in these studies are listed in Table 1. Cells were grown at 30°C in rich minimal medium (0.67% yeast nitrogen base without amino acids, 2% casamino acids, and 2% glucose or 2% galactose) with the appropriate supplements: adenine (30 μg/ml), histidine (20 μg/ml), lysine (40 μg/ml), and methionine (20 μg/ml). Cells were grown overnight at 30°C to stationary phase, then diluted to ~0.1 OD_{600}/ml in appropriate medium and sampled at subsequent time points. The cells with the green fluorescent protein (GFP) fusions were grown overnight in rich minimal medium with 3% raffinose and 10× adenine in addition to the usual supplements, and then diluted into the same media containing 2% galactose and 3% raffinose and grown for at least 12 h at 30°C. For semi-anaerobic growth conditions, cells were inoculated into a small flask filled to the top with medium, sealed with parafilm, and incubated at 30°C. Lovastatin was prepared as described (Hampton and Rine, 1994) and was used at 50 μg/ml.

Plasmids

The multicopy (2 micron) plasmids containing *HMG1* (pJR59) and *HMG2* (pJR360) have been previously described (Basson *et al.*, 1986; Wright *et al.*, 1988). The galactose-inducible *HMG1* construct (pAK266) was a subclone of pJR435 (Basson *et al.*, 1988). Using standard techniques (Maniatis *et al.*, 1982), a 0.7-kb *Eco*RI–*Sal*I fragment of DNA containing the *GAL1/10* promoter from pJR435 was ligated into pRS306 (Sikorski and Hieter, 1989), which was digested with the same enzymes, producing pAK85. A 3.7-kb *Sal*I fragment containing the *HMG1* gene with no 5′-untranslated region was placed into the *Sal*I site of pAK85 to yield pAK107. Finally, pAK107 was digested with *Xho*I and *Not*I to yield a 4.4-kb fragment containing the *HMG1* gene under control of the *GAL1* promoter, and the fragment was ligated into pRS316 (Sikorski and Hieter, 1989) digested with the same enzymes, yielding pAK266. The galactose-inducible *HMG2* construct pRH134-2 was provided by Randy Hampton (University of California Berkeley, Berkeley, CA). pRH134-2 was made by placing a *Pst*I–*Sal*I fragment containing *HMG2* (Hampton and Rine, 1994) 3′ of the *GAL1* promoter in pJR168 (Basson *et al.*, 1988), which had been digested with *Bam*HI and *Sal*I. The two fragments were connected using a *Bam*HI–*Pst*I adapter (NEB, Beverly, MA). The Hmg2p chimeric construct (pMP375) containing the Loop G of Hmg1p has been previously described (Parrish *et al.*, 1995).

The GFP (Prasher *et al.*, 1992; Chalfie *et al.*, 1994) expression constructs used in these studies were derived from the plasmid pJC81 (provided by Jeff Cox and Peter Walter, UCSF, San Francisco,

Table 1. Yeast strains

Strains		Reference
JRY527	MATa HMG1 HMG2 ura3-52 his3Δ200 ade2-101 lys2-801 met	Basson *et al.*, 1986
JRY1239	MATa HMG1 HMG2 ura3-52 his3Δ200 ade2-101 lys2-801 met pJR59 (multicopy HMG1)	Basson *et al.*, 1986
RWY306	MATa HMG1 HMG2 ura3-52 his3Δ200 ade2-101 lys2-801 met pJR360 (multicopy HMG2)	This paper
JRY1159	MATa hmg1::LYS2 HMG2 ura3-52 his3Δ200 ade2-101 lys2-801 met	Basson *et al.*, 1986
JRY1160	MATa HMG1 hmg2::HIS3 ura3-52 his3Δ200 ade2-101 lys2-801 met	Basson *et al.*, 1986
RWY410	MATa HMG1 HMG2 ura3-52 his3Δ200 ade2-101 lys2-801 met pAK266 (pGAL1-HMG1)	This paper
RWY446	MATa HMG1 HMG2 ura3-52 his3Δ200 ade2-101 lys2-801 met pRH134-2 (pGAL-HMG2)	This paper
RWY590 (same as 591)	MATα HMG1 HMG2 leu2-3 leu2-112 prc1::LEU2 suc2Δ9 ura3-52 pMP375 (multicopy HMG2 with Loop G of HMG1)	Parrish *et al.*, 1995
RWY605	MATα HMG1 HMG2 leu2-3 leu2-112 prc1::LEU2 suc2Δ9 ura3-52 pJR360 (multicopy HMG2)	Parrish *et al.*, 1995
RWY621	MATa HMG1 HMG2 ura3-52 his3Δ200 ade2-101 lys2-801 met pCR425 (pGAL Hmg1:GFP)	This paper
RWY663	MATa HMG1 HMG2 ura3-52 his3Δ200 ade2-101 lys2-801 met pAK443 (pGAL Hmg2:GFP)	This paper

CA). This plasmid contains a mutant version of *GFP10* in which the first two codons have been changed to encode a *Bam*HI site. To provide restriction sites useful for constructing in-frame gene fusions, a 1.2-kb *Bam*HI–*Sal*I fragment of pJC81 (containing the 710-bp *GFP10* open reading frame, 400 bp of the *ACT1* gene containing the transcriptional terminator, and 90 bp of the *tet* gene) was subcloned into the *Bam*HI–*Sal*I sites of pALTER-1 (Promega, Madison, WI), creating plasmid pCR416. This positioned *Kpn*I and *Sma*I sites upstream of the *Bam*HI site. A 1.2-kb *Kpn*I–*Sal*I fragment was ligated to the 8.4-kb *Kpn*I–*Xho*I fragment of pAK266, creating plasmid pCR425. This created an Hmg1:GFP fusion, encoding the *GAL1/10* promoter, N-terminal 987 amino acids of Hmg1p (deleting the 67 C-terminal residues), followed by two linker residues and all of GFP except for the initiating methionine. The Hmg2:GFP fusion was made by placing a 3.4-kb *Eco*RI–*Bam*HI fragment of pRH134-2 containing the *GAL1/10* promoter and 893 codons of *HMG2* (deleting the 152 C-terminal codons) into the *Eco*RI and *Bam*HI sites of pCR416, to create an in-frame fusion with GFP called pAK442. A 4.6-kb *Eco*RI–*Sal*I fragment of pAK442 containing the Hmg2:GFP fusion was placed into the yeast vector pRS316 at its *Eco*RI and *Sal*I sites, creating pAK443.

DiOC6 Staining and Confocal Microscopy

$DiOC_6$ (3,3′-dihexyloxacarbocyanineiodide) staining was performed as previously described (Koning *et al.*, 1993). Briefly, a 10 mg/ml or 1 mg/ml stock solution of $DiOC_6$ (Kodak, Rochester, NY) dissolved in ethanol was used to stain cells at a final concentration of 10 μg $DiOC_6$/1 OD_{600} cells. Cells (2 μl) stained with $DiOC_6$ were spread thinly on a slide and immobilized with 5 μl of 1% Sea Plaque agarose (FMC Bioproducts, Rockland, ME) dissolved in medium, and covered with a coverslip. Stained cells were observed with either conventional fluorescence optics, using a Nikon Microphot-FXA epifluorescence microscope with excitation (480 ± 20 nm) and barrier (535 ± 40 nm) filters appropriate for fluorescein, or confocal microscopy, using a Bio-Rad MRC600 confocal microscope (Richmond, CA) with a 488 nm excitation wavelength and the BHS emission filter. Images were collected using a laser emission of 0.1% transmittance, with the aperture set to give an approximate optical section of 0.5 μm.

Electron Microscopy

Preparation of cells for electron microscopy and immuno-electron microscopy was a variation on methods previously described (Wright and Rine, 1989). Specifically, for conventional electron microscopy, cells were grown to 1 OD_{600}/ml and 40 ml of culture was fixed in 2% glutaraldehyde in buffer (0.1 M Trizma base, 10 mM KCl, 0.54 M NaCl, 1 mM $CaCl_2$, 1 mM $MgCl_2$, 0.2 M sorbitol), then postfixed in 2% $KMnO_4$, and stained *en bloc* with 1% uranyl acetate. The cells were dehydrated through a graded ethanol series, and embedded in Pelco Ultra Low Viscosity resin (Ted Pella, Redding, CA) as previously described. Alternatively, cells in which the position of karmellae relative to the nucleolus was scored were prepared by fixation in glutaradehyde and 2% OsO_4 as previously described (Byers and Goetsch, 1991). Sections were prepared as previously described (Wright and Rine, 1989) and stained with Reynold's lead citrate (Reynolds, 1963). Observations were made on a Philips 300 or a CM100 microscope at 60-80 kV.

For immuno-electron microscopy, cells were grown to stationary phase in glucose medium, washed, and resuspended at ~0.1 OD_{600}/ml in galactose medium, and grown for 12 h. Again, 40 ml of cells were fixed in 1% EM grade glutaraldehyde, and 1% EM grade formaldehyde (Ted Pella) in 40 mM potassium phosphate (pH 6.8). The cells were treated with 1% aqueous sodium metaperiodate, and 50 mM ammonium chloride as described. The cells were dehydrated through a graded ethanol series and embedded in LR White Resin medium grade (Ted Pella). The resin was polymerized at 47°C for 2 days, and then sections were cut with a diamond knife and mounted on 200 mesh nickel grids. Before treatment with antisera, grids were heated at 60°C for 2 min to ensure that the sections would not come off during subsequent incubations and washes. For immunostaining, grids were treated as previously described (Wright and Rine, 1989). Blocking solution contained PBST (140 mM NaCl, 3 mM KCl, 8 mM Na_2HPO_4, 1.5 mMKH_2PO_4, 0.5% Tween-20), 1% ovalbumin grade VII (Sigma Chemical, St. Louis, MO), and 0.1% cold water fish gelatin (Amersham, Arlinton Heights, IL). Hmg2p was detected using a 1:100 dilution of an antibody (2970) generated against the C-terminal 15 amino acids of Hmg2p. This antibody does not cross-react with Hmg1p. Sections were treated similarly with pre-immune serum. The goat-anti rabbit secondary antibody coupled to 10-nm gold particles (Ted Pella) was diluted to 0.13 OD_{520} in blocking solution. After immunostaining, sections were either stained with 2% uranyl acetate and Reynold's lead citrate, or left unstained, and observed using a Philips CM100 electron microscope at 60-80 kV.

Immunofluorescence

Immunofluorescence was performed using a procedure similar to that described by Pringle *et al.* (1989). Log phase cells were fixed in 3.7% formaldehyde for 1 h at room temperature. The cells were centrifuged for 3 min at 834 × *g* in a clinical centrifuge, resuspended in 2 ml solution B (1 M potassium phosphate buffer, pH 7.5, 1.2 M sorbitol), and stored at 4°C. Two OD_{600} units of cells were washed twice in 1 ml solution B, resuspended in 900 μl solution B, and split into two 450-μl aliquots. Fifty microliters of a mix of digestion enzymes (50 μl of 1 mg/ml zymolyase 20T [ICN, Costa Mesa, CA]), 50 μl glusulase >10 U/μl [NEN, DuPont Company, Wilmington, DE], and 5 μl β-mercaptoethanol) was added to each sample, which was then incubated at 37°C for 10 and 15 min, respectively. After cell wall digestion, the cells were washed twice with 1 ml cold (4°C) TBS (25 mM Trizma base, 3 mM KCl, 140 mM NaCl). Finally, the cells were resuspended in 0.5 ml TBS. Fifteen microliters of the cell suspension was loaded onto each well of a multiwell slide (Cel-Line Associates, Newfield, NJ) that had been pre-treated with 0.5% polyethylenimine for 1-2 min (Sigma Chemical). The cell suspension sat on the slides for 20 min in a humidified box, and then nonadherent cells were very gently rinsed away three times with a drop of TBS applied from a pasteur pipette and an aspirator. Cells were blocked with 10 μl of filtered (0.22 μm) block solution (TBS + 0.05% Tween 20), 1% ovalbumin Grade VII (Sigma Chemical)] for 30 min at room temperature. Primary antibodies were diluted in block solution to 2× the desired final concentration and centrifuged for 15 min at 4°C before use. Antibodies generated against the divergent C-terminal 15 amino acids of Hmg1p (DINRLKDGSVTCIKS) and Hmg2p (QPSNKGPPCKTSALL) were used at 1:20 to 1:100 final concentrations. Kar2p antiserum was a gift of Mark Rose (Princeton University, Princeton, NJ) and was used at a 1:2000 dilution. Sec61p antiserum was a gift of Jeff Brodsky (University of Pittsburgh, Pittsburgh, PA), and was used at a 1:500 dilution. Ten microliters of 2× primary antibody was applied directly to the block solution already present in the well and incubated at room temperature for 1 h. The antibody solution was gently aspirated away, and the cells washed five times with TBST. Again 10 μl of blocking solution was applied to each well. Ten microliters of secondary antibody (goat anti-rabbit fluorescein conjugated or donkey anti-rabbit Texas Red conjugated; Cappel Organon Technika, Durham, NC) was diluted 1:500 or 1:250 in block solution, centrifuged for 15 min, and applied to each well. After 45 min, the 2° antibody was washed five times with TBST. Ten microliters of 1 μg/ml 4,6-diamidino-2-phenylindole (DAPI; Sigma Chemical) in TBS was added to each well for 1 min. After one rinse with TBS, a drop of Citifluor (Ted Pella) was applied to each well, and the slide sealed with a coverslip and nailpolish. Each experiment typically included treatment of a sample with an antibody to detect tubulin (Yol1/34; 1:10 dilution; Accurate Chemical and Scientific Company, Westbury, NY) as a positive control.

Immunoprecipitation

HMGR protein was immunoprecipitated using a procedure similar to that described by Hampton and Rine (1994) and Sengstag *et al.* (1990). Cells that had been growing in galactose medium for 11.5 h were pelleted for 5 min at 834 × *g* in a clinical centrifuge, washed with 1 ml galactose medium with no casamino acids or methionine supplement, repelleted, and finally resuspended at approximately the original starting OD_{600} in galactose medium with no casamino acids or methionine. The cells were labeled at 30°C for 30 min with 50 μCi Tran^{35}S-label (NEN)/OD_{600} of cells. The labeled cell pellets were stored at −76°C until processed. A total membrane fraction was prepared from the labeled cells using modifications of a method previously described (Deschenes and Broach, 1987). The frozen cell pellet was thawed on ice in 1 ml lysis buffer [0.3 M sorbitol, 0.1 M NaCl, 5 mM $MgCl_2$, and 20 mM 3-(*N*-morpholino)propanesulfonic acid, pH 7.4] containing protease inhibitors [2 μg/ml each TPCK (*N*-tosyl-L-phenylalanine chloromethyl ketone), leupeptin, pepstatin A, aprotinin (Sigma Chemical), and 1 mM PefaBloc SC (Boehringer Mannheim Biochemica, Indianapolis, IN)]. Cells were pelleted and resuspended in 100 μl lysis buffer with protease inhibitors in a screw cap Eppendorf tube. Acid-washed glass beads were added up to the meniscus and the sample was agitated for 80 s using a Mini-Beadbeater (Baxter, Redmond, WA) at 4°C. To maximize recovery of lysate after beadbeating, several holes were made in the cap of the microcentrifuge tube with a 25G needle, and the tube was placed upside down in a 15-ml conical plastic tube (Lum and Wright, 1995). The lysate was removed from the beads by centrifugation at 834 × *g* for 5 min in a clinical centrifuge at 4°C. The entire sample was transferred to a screw-cap Eppendorf tube and microcentrifuged at 4°C for 20 min at top speed. The pelleted membranes were resuspended in 75 μl SUTE/OD_{600} (1% SDS, 8 M urea, 10 mM Tris, pH 7.5, 10 mM EDTA) and heated at 65°C for 10 min. Then, 400 μl of IPB (15 mM NaH_2PO_4, pH 7.5, 150 mM NaCl, 2% Triton X-100, 0.1% SDS, 0.5% deoxycholate) with protease inhibitors was added to equivalent samples in 75 μl of SUTE, which was then pre-cleared with 50 μl of a 10% w/v solution of protein A-Sepharose CL-4B beads (equilibrated and de-fined in IPB; Pharmacia Diagnostics, Fairfield, NJ). After rotating 30 min at 4°C, the samples were briefly centrifuged to pellet the beads. The supernatant was transferred to a new tube to which 15 μl of a polyclonal anti-β-galactosidase-Hmg1p antiserum was added (Wright and Rine, 1989). This antiserum also recognizes the Hmg2p isozyme, albeit with less affinity. After rotating 5 h at 4°C the samples were left stationary overnight. The next day, 50 μl of CL-4B beads were added, and the sample was rotated at 4°C for 3-4 h. After a brief centrifugation, the supernatant was transferred to a new tube to which 15 μl more antibody was added for a second round of immunoprecipitation. The beads were washed three times with 500 μl IPB, then once with 10 mM Tris (pH 7.5), 50 mM NaCl. Finally, the beads were heated at 65°C for 10 min in 30 μl 2× urea sample buffer (8 M urea, 4% SDS, 10% β-mercaptoethanol, 0.125 M Tris, pH 6.8). The second and third rounds of immunoprecipitations with the same supernatant were treated with CL-4B beads as described. After electrophoresis through a 7.5% polyacrylamide gel with a 3% stacker, the dried gel was analyzed with a PhosphorImager (Molecular Dynamics, Sunnyvale, CA) and was also autoradiographed using Kodak X-AR film.

RESULTS

Increased Levels of Hmg1p and Hmg2p Induced the Proliferation of Distinct Sets of Membranes

Yeast cells respond to increased levels of Hmg1p by proliferating stacked pairs of nuclear-associated membranes called karmellae, a term that reflects the position of the proliferated ER membranes near the nucleus and their lamellar appearance (Wright *et al.*, 1988). We can rapidly assay living cells at various stages of growth for the presence of membrane proliferations by using the positively charged, lipophilic molecule $DiOC_6$ (Koning *et al.*, 1993). As expected, $DiOC_6$ staining of cells containing a multicopy *HMG1* plasmid (pJR59) revealed the presence of karmellae membranes. A comparison of the membrane proliferations in these yeast cells observed with confocal microscopy of $DiOC_6$-stained cells and with electron microscopy is shown in Figure 1. Nuclear-associated karmellae membranes are compared in Figure 1, A and B (arrows). Cells with high levels of Hmg1p also occasionally contained other types of membrane proliferations such as peripherally located, closely stacked pairs of membranes called strips, and concentric multi-layered membrane whorls (Figure 1, C–F, arrows; see also Lum and Wright, 1995). However, these membrane proliferations were typically present only in combination with karmellae membranes. In rare cases, strips appeared by themselves early in the growth phase. In addition, whorls accumulated late in the growth phase.

$DiOC_6$ staining and electron microscopy of cells containing a multicopy *HMG2* plasmid (pJR360) revealed the presence of membrane proliferations that were distinct from those induced by increased levels of Hmg1p. Although both Hmg1p- and Hmg2p-induced membrane proliferations consisted of closely stacked pairs of membranes, the morphology and abundance of the Hmg2p membrane proliferations were different from those induced by increased levels of Hmg1p. Instead of displaying the typical Hmg1p type "half-moon" karmellae that usually curve over one-half to three-quarters of the nucleus, Hmg2p induced the proliferation of peripherally located strips, whorls, and "short" karmellae that covered only one-eighth to one-third of the nucleus (Figure 2, A and B, arrows). These short karmellae frequently appeared to flatten the nucleus, both in $DiOC_6$-stained living cells and in cells fixed for electron microscopy. Unlike karmellae induced by increased levels of Hmg1p, short karmellae were not the most abundant type of Hmg2p-induced membrane proliferation. Instead, the majority of cells contained multiple strips or whorls either alone or in combination (Figure 2, C–F, arrows).

Since both Hmg1p and Hmg2p could induce the proliferation of nuclear-associated membranes, we analyzed whether these membranes showed a preferential orientation on the nucleus or whether the membranes proliferated randomly. We used the nucleolus as an orientation marker because the yeast nucleus contains a higher order structure such that the spindle pole body lies opposite the nucleolus (Yang *et al.*, 1989). Strikingly, the nuclear-associated membranes were most often located on the side of the nucleus containing the nucleolus (Figure 3). Additionally, cells with karmellae had an enlarged zone of densely stain-

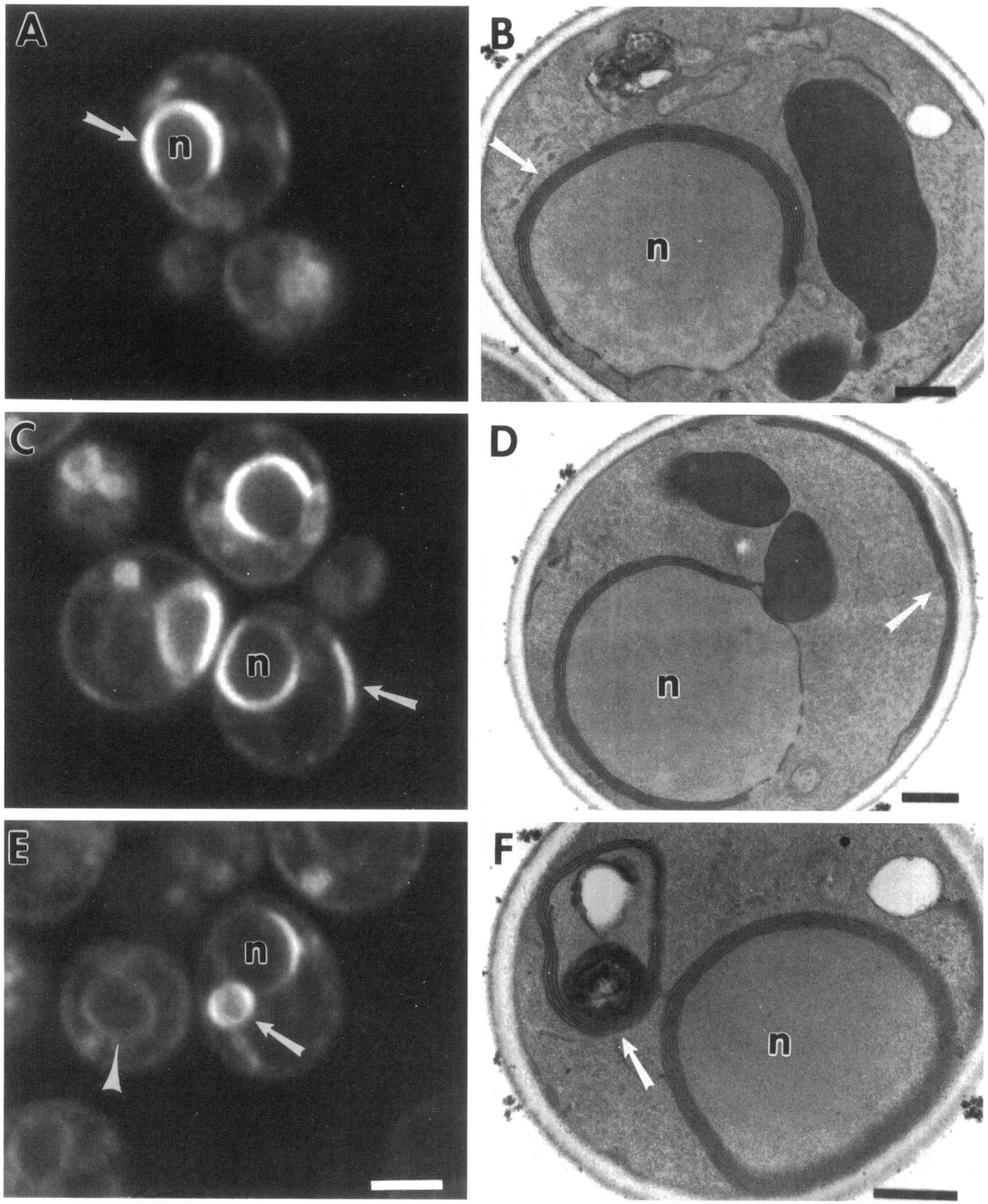

Figure 1. Membrane proliferations induced by increased levels of the Hmg1p isozyme. Representative cells of strain JRY1239 with Hmg1p-induced membranes are shown. Mid-log phase cells containing a multicopy *HMG1* plasmid (pJR59) were either stained with the lipophilic dye $DiOC_6$ and examined by confocal microscopy (A, C, and E) or fixed for electron microscopy (B, D, and F). (A and B) Hmg1p induces the proliferation of karmellae membranes (arrow) associated with the nucleus (n). (C and D) Cells with karmellae and additional

ing material associated with the nucleolus (Figure 3A, arrow) as previously observed (Wright *et al.*, 1988). A smaller area of densely staining material was observed in both wild-type cells and in cells with short karmellae (Figure 3, B and C, arrows).

Hmg2p-induced Membranes Disappeared Faster than Hmg1p-induced Membranes

A direct comparison of membrane proliferations from expression of the isozymes on multicopy plasmids was complicated by the differential regulation of the *HMG1* and *HMG2* promoters (Thorsness *et al.*, 1989). Therefore, to control for differences in the HMGR promoters, cells expressing *HMG1* or *HMG2* under control of a galactose-inducible promoter (*GAL1*) were compared.

In both cases, membrane proliferations triggered by increased amounts of the two HMGR isozymes first arose 2-4 h after induction of the *GAL1* promoter and steadily increased in the population until 12 h after induction (Figure 4A). Over this time period, cells with increased levels of Hmg1p accumulated membrane proliferations in an average of 46% of the cells. The majority of membrane proliferations in these cells were karmellae (Figure 4B), and peripheral strips and whorls were most often found in cells that already had karmellae membranes. In fact, cells containing only proliferations of peripheral ER strips were rarely seen. Following the peak of membrane proliferation at 12 h after induction, the number of cells with either Hmg1p or Hmg2p membrane proliferations declined over the following 66 h. Whorls became more evident in both the Hmg1p and Hmg2p cultures during late log and stationary phase (Figure 4B). In Hmg1p-induced cultures, whorls increased from 1 to 8.5% between 24 to 48 h after induction, but karmellae still remained a major form of proliferation (9.6%) even at 48 h.

Hmg2p-induced membrane proliferations also steadily increased between 4-12 h after induction, peaking with an average of 40% of the cells containing membrane proliferations. Cells with high levels of Hmg2p accumulated short karmellae (9.8%), whorls (8.6%), or single or multiple strips (14.3%) in approximately equal abundance in the first half of the time course (Figure 4B). Between 24 and 30 h after induction, the percent of cells containing Hmg2p-induced membranes declined at a threefold faster rate than the percent of cells containing Hmg1p-induced membranes (Figure 4A). In addition, as the number of cells with Hmg2p-induced proliferations declined over the second half of the time course, whorls and strips (9.6% and 13.6%) became the major forms of proliferation, and short karmellae became a minor form of proliferation (2.8%) (Figure 4B, 24 h).

Differences in Protein Amounts Did Not Account for the Different Types of Membranes Proliferated in Response to the Two Isozymes

To investigate whether the different sets of membrane proliferations produced in response to high levels of Hmg1p and Hmg2p were due to differences in the steady state levels of these proteins, we compared levels of the HMGR isozymes at 12 h following induction of the *GAL1* promoter, at the peak of membrane proliferations. Both Hmg1p and Hmg2p were immunoprecipitated using a polyclonal antiserum generated against the catalytic domain of Hmg1p (Wright *et al.*, 1988). This antiserum also cross-reacts with the Hmg2p catalytic domain, although with less affinity. To ensure that all the HMGR protein was immunoprecipitated, the samples were subjected to multiple rounds of immunoprecipitation (Figure 5A). Quantification of the immunoprecipitations using PhosphorImager analysis revealed that the Hmg1p and Hmg2p protein levels were similar (Figure 5B). In fact, the Hmg2p levels were slightly higher than the Hmg1p levels. This result indicated that the different types of membranes proliferated in response to the different HMGR isozymes were not due to variations in the amount of the respective proteins in the cell.

Increasing the Stability of Hmg2p with Lovastatin Increased the Abundance of Membrane Proliferations, but Did Not Change their Morphology

A major difference between Hmg1p and Hmg2p is the relative stability of the two proteins. Since Hmg2p has a much shorter half-life than Hmg1p (Hampton and Rine, 1994), it is possible that the different types of membranes proliferated in response to Hmg2p may simply reflect Hmg2p's decreased stability. If this is the case, stabilizing Hmg2p should produce a profile of membrane proliferations similar to those induced by the more stable Hmg1p. To test this possibility, we took advantage of the ability of low amounts of lovastatin, a competitive inhibitor of HMGR, to stabilize Hmg2p, thus lengthening its half-life to more resemble that of Hmg1p (Hampton and Rine, 1994). The low amount of lovastatin used in these experiments (50 μg/ml) had only a slight effect on the growth rate of the culture, increasing the doubling time from 227 to 250 min.

Interestingly, stabilizing Hmg2p with lovastatin did not change the types of membranes produced in re-

(Figure 1 cont.) proliferations of peripheral ER membranes called strips (arrow). (E andF) Cells with karmellae and additional membrane proliferations called whorls (arrow). Also shown in panel E is a cell with no visible Hmg1p-induced membrane proliferations (arrowhead). Bar for panels A, C, and E, 2 μm; and for panels B, D, and F, 500 nm.

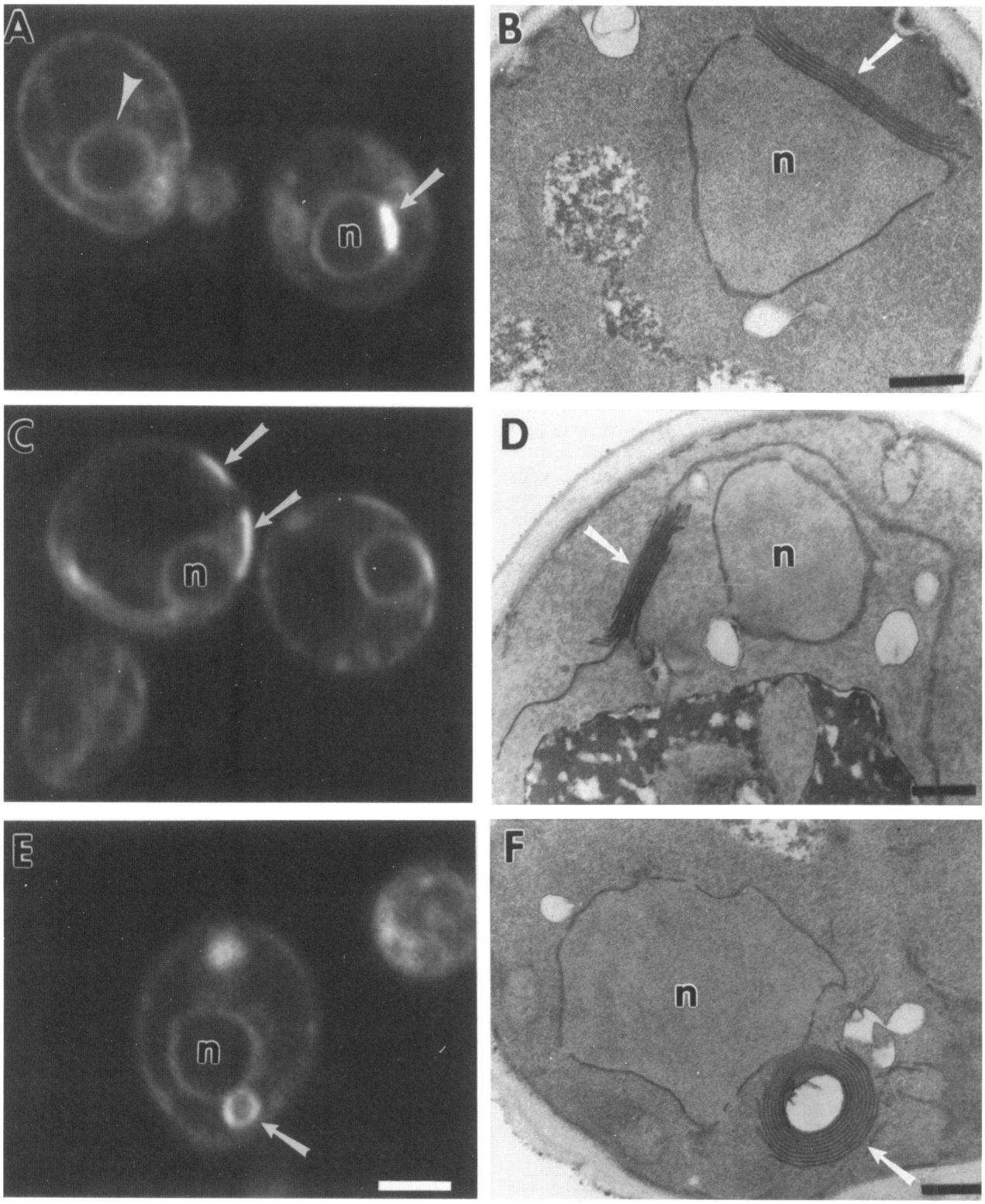

Figure 2. Membrane proliferations induced by increased levels of the Hmg2p isozyme. Representative cells of strain RWY306 with Hmg2p-induced membranes are shown. Mid-log phase cells containing a multicopy *HMG2* plasmid (pJR360), were either stained with the lipophilic dye $DiOC_6$ and examined by confocal microscopy (A, C, and E) or fixed for electron microscopy (B, D, and F). (A and B) Hmg2p induced the proliferation of "short" karmellae membranes (arrow) associated with the nucleus (n). Also shown in panel A is a cell with no

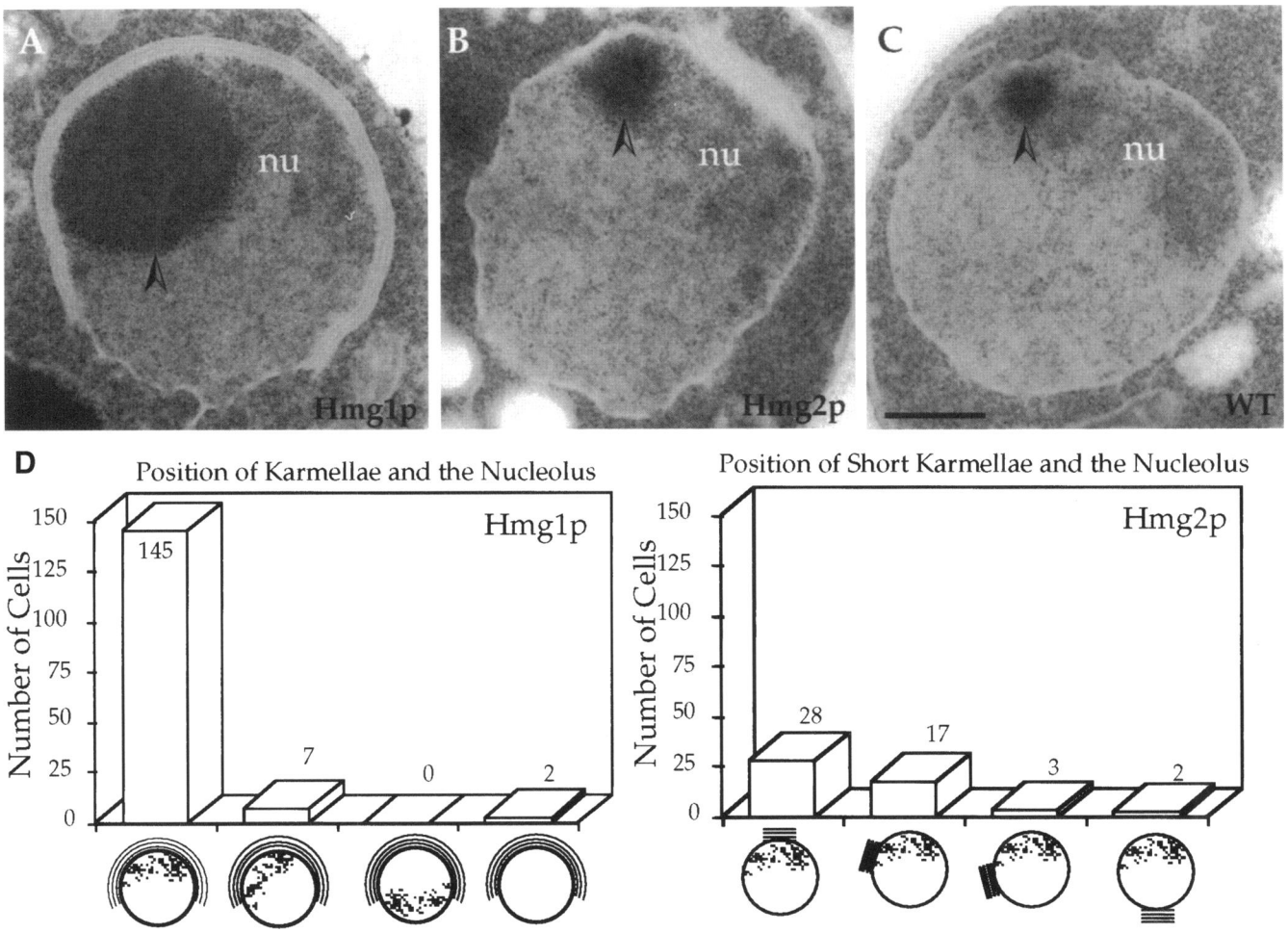

Figure 3. Position of nuclear-associated membranes relative to the nucleolus. (A) A representative nucleus in strain JRY1239 (multicopy *HMG1*) with prominent karmellae membranes. Karmellae were most often located on the nucleolar side of the nucleus. A densely stained area associated with the nucleolus (nu) is indicated by an arrowhead. (B) A nucleus with short karmellae in strain RWY306 (multicopy *HMG2*) is shown. Short karmellae were also most often located on the nucleolar side of the nucleus. A densely stained area of the nucleolus (nu) is indicated by an arrowhead). (C) A nucleus in a wild-type cell strain (JRY527) is shown for comparison. A densely stained area of the nucleolus (nu) is indicated by an arrowhead. (D) The position of each type of karmellae membrane was tabulated in relation to the position of the nucleolus in sections of cells prepared for electron microscopy. The nucleolus is represented by the stippled area in the pictoral representations, and the karmellae membranes by the lines around part of the nucleus. Only sections in which karmellae did not entirely encompass the nucleus or in which the nuclei were not undergoing mitosis were scored. Bar, 500 nm.

sponse to increased levels of Hmg2p. Short karmellae, strips, and whorls were still formed. However, the number of cells with membrane proliferations in the lovastatin-stabilized culture remained high even after the Hmg2p membrane proliferations in the untreated culture had declined (Figure 6A). This effect was especially apparent at 53 h when 45% of the cells treated with lovastatin still contained membrane proliferations compared with only 3.5% of the cells in the control culture without lovastatin. The persistence of membrane proliferations in the lovastatin-stabilized Hmg2p culture resembled the persistence of Hmg1p-induced membrane proliferations. Another difference evident in the Hmg2p culture with lovastatin was that short karmellae persisted after they normally would have represented a minor type of membrane proliferation (Figure 6B, 24 h). However, peripheral strips and whorls still formed a sizable fraction of the types of membranes proliferated.

(Figure 2 cont.) visible Hmg2p-induced membrane proliferations (arrowhead). (C and D) Cells with increased levels of Hmg2p containing proliferations of peripheral ER membranes called strips (arrow). (E and F) Cells with whorls of membranes (arrow). Bar for panels A, C, and E, 2 μm; and for panels B, D, and F, 500 nm.

The altered distribution of membrane proliferations in the Hmg2p culture treated with lovastatin suggested that the persistence of Hmg1p-induced membranes in late log and stationary phase may reflect the stability of this isozyme, because membrane proliferations also persisted in the cells with lovastatin-stabilized Hmg2p. However, the differences in the types of membrane proliferations produced in response to the two isozymes were not changed by stabilizing the Hmg2p isozyme, and therefore could not be explained by the differential stability of Hmg1p versus Hmg2p. Instead, the same types of membrane proliferations were produced by the Hmg2p cultures plus or minus lovastatin. Consequently, the differences in the types of membrane proliferations induced by increased levels of Hmg1p or Hmg2p were intrinsic to the different isozymes, and reflected the different subcellular distributions of the two proteins.

Increased Levels of Hmg1p and Hmg2p Had Distinct ER Localization Patterns

In cells with a 10-fold increase in Hmg1p levels, the protein is present in karmellae membranes (Wright *et al.*, 1988). Previously, the subcellular location of Hmg1p expressed at endogenous levels could not be determined, because HMGR is not an abundant protein. Even when overexpressed, Hmg1p is estimated to make up less than 0.1% of the total cellular protein (Wright *et al.*, 1988). However, by optimizing the protocol for detection of HMGR, we determined the subcellular localization of endogenous levels of Hmg1p using indirect immunofluorescence with an antibody that specifically recognizes the C-terminus of the Hmg1p isozyme. Endogenous levels of Hmg1p were localized predominantly in the nuclear envelope in a strain deleted for the Hmg2p isozyme (Figure 7, A and B). The same localization of Hmg1p was found in a wild-type strain expressing both isozymes (our unpublished results). For comparison, the localization of a lumenal ER protein Kar2p, which is present throughout the ER, is shown in Figure 7, C and D (Rose *et al.*, 1989; Preuss *et al.*, 1991).

In cells containing a multicopy *HMG1* plasmid, Hmg1p was found predominantly in the nuclear envelope, although some additional peripheral ER staining was detectable as assayed by indirect immunofluorescence (Figure 7, E and F). This localization coincided with the proliferation of membranes induced by increased levels of Hmg1p: karmellae membranes arose around the nucleus, and strips arose at the cellular periphery, presumably from the ER at this location. In cells with elevated levels of Hmg1p, Kar2p staining was also seen in thickened areas of the nuclear envelope that are presumably karmellae (Figure 7, G and H). The variation in staining intensity of Hmg1p may reflect differences in the number of plasmids inherited by the cell (Rose and Broach, 1991), as well as differential inheritance of karmellae membranes that segregate with the mother cell (Wright

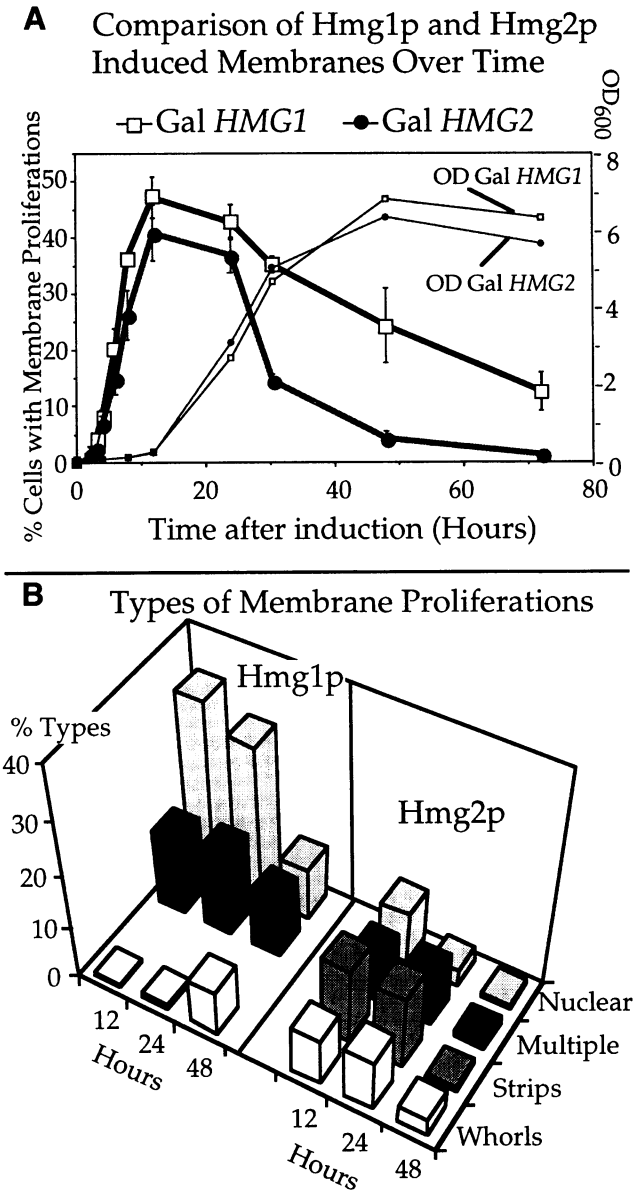

Figure 4. Comparison of membrane proliferations induced by either Hmg1p or Hmg2p. Cells containing either a galactose-inducible *HMG1* (RWY410) or a galactose-inducible *HMG2* (RWY446) were grown to stationary phase in glucose medium, and then diluted into fresh galactose media to induce the production of Hmg1p or Hmg2p. (A) The average amount of total Hmg1p- or Hmg2p-induced membrane proliferations at various timepoints is plotted. Each point represents an average amount of membrane proliferations (± standard error) from four to six separate experiments. In each experiment, at least 200 cells were scored per timepoint. Also shown is a representative growth curve. (B) The relative abundance of the different types of membrane proliferations seen at three different timepoints is compared for the Gal *HMG1* and Gal *HMG2* cultures.

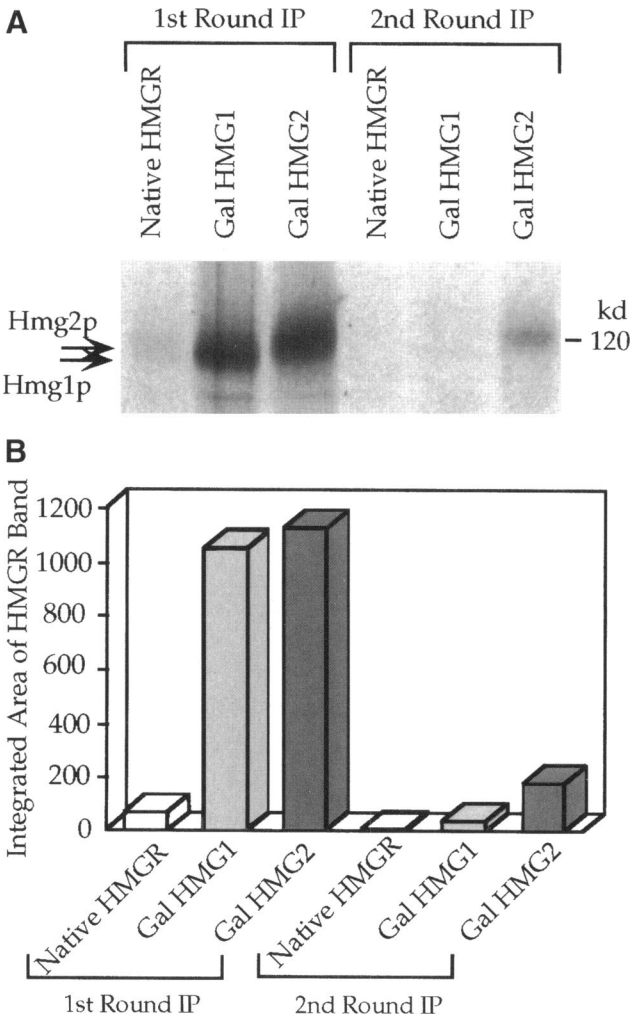

Figure 5. Comparison of Hmg1 and Hmg2 protein levels by immunoprecipitation. Cells containing either native levels of HMG-CoA reductase (JRY527), the Gal HMG1 (RWY410), or the Gal HMG2 construct (RWY446) were labeled at the 12 h peak of membrane proliferations and the protein was immunoprecipitated. A polyclonal antisera raised against a fusion of the catalytic domain of Hmg1p fused to lacZ was used to immunoprecipitate both Hmg1p and Hmg2p. Two rounds of immunoprecipitations were performed to ensure that all the HMG-CoA reductase (HMGR) was precipitated. (A) Autoradiograph of the immunoprecipitation showing precipitation of Hmg1p and Hmg2p (arrowheads). Hmg2p runs slightly higher than Hmg1p. Additional Hmg2p was immunoprecipitated in the second round. (B) The amount of signal immunoprecipitated was quantified using a PhosphorImager.

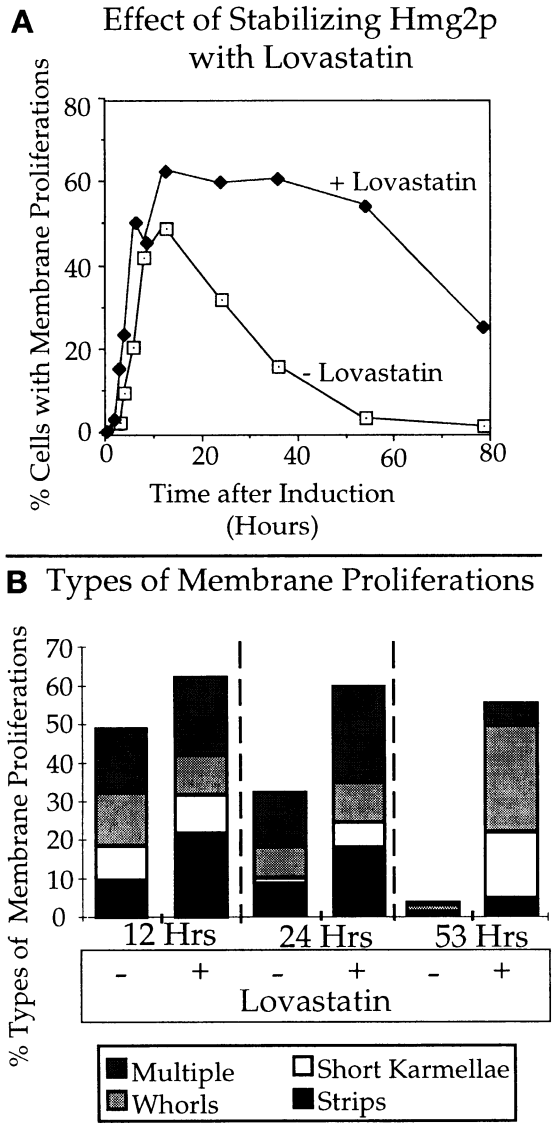

Figure 6. Stabilizing the Hmg2p with lovastatin did not change the types of membranes proliferated in response to this isozyme, but did change their relative abundance. Cells (RWY446) containing the Gal *HMG2* construct were grown in glucose overnight, diluted into fresh galactose media, and then split into two identical cultures. Lovastatin (50 μg/ml) was added to one of the cultures. Total % cells with membrane proliferations and the types of membrane proliferations were scored in at least 200 cells per timepoint. (A) Total % cells with membrane proliferations in the cultures ± lovastatin over time. (B) A comparison of the different types of Hmg2p-induced membranes proliferated in the presence or absence of lovastatin at three time points.

et al., 1988). In the figure, Kar2p staining appears brighter in cells with increased levels of Hmg1p versus cells with endogenous levels of Hmg1p. However, this difference simply represents variation between experiments, not elevated levels of Kar2p. In fact, quantitative immunoblots demonstrated that Kar2p is not induced by Hmg1p overproduction (Wright, Koning, Parrish, unpublished results; Jeff Brodsky, personal communication).

Based on enzyme activity assays in cells deficient for one or the other HMGR isozyme, Hmg2p contributes less than a quarter of the HMGR activity in yeast cells grown aerobically (Basson *et al.*, 1986). Thus, Hmg2p

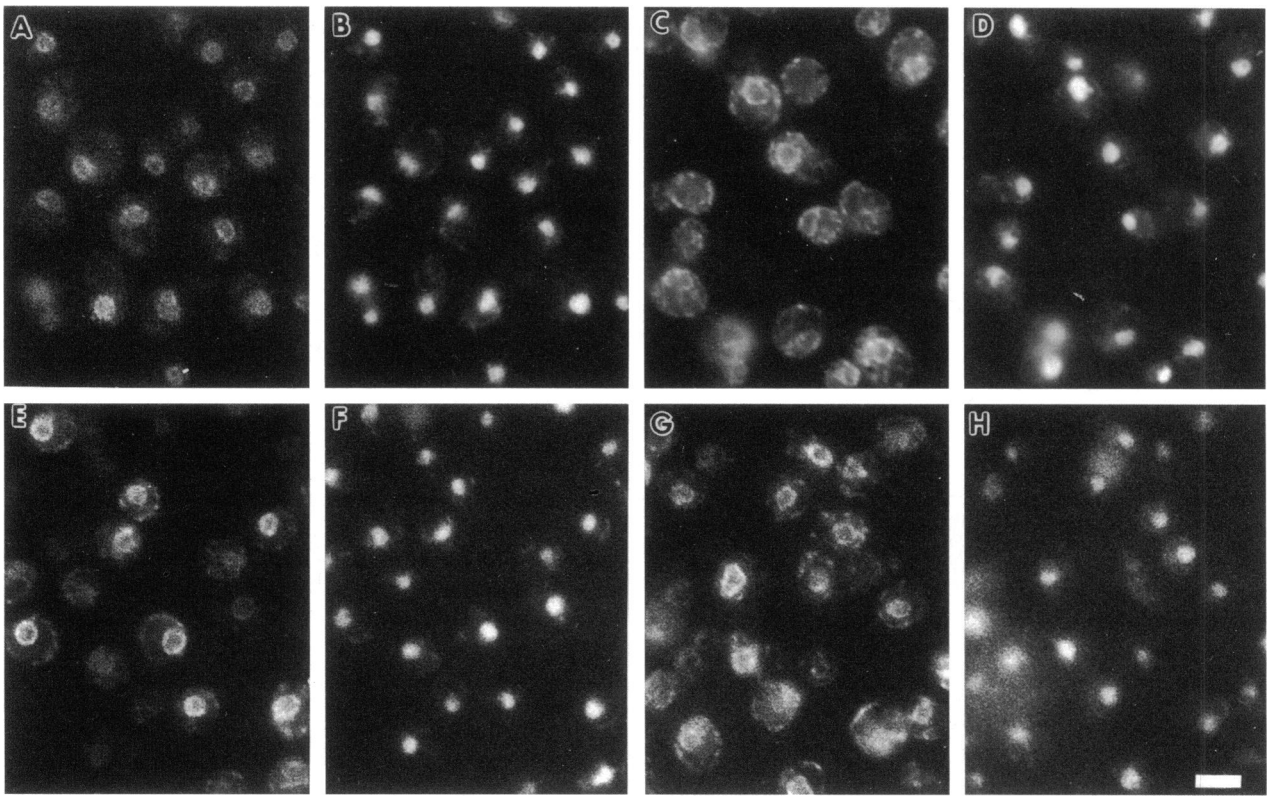

Figure 7. Localization of endogenous and increased levels of Hmg1p by indirect immunofluorescence. Indirect immunofluorescent localization of Hmg1p and Kar2p is shown in panels A, C, E, and G. Localization of the nucleus in the same cells is shown by DAPI staining in panels B, D, F, and H. (A and B) Localization of endogenous levels of Hmg1p was determined in cells of strain JRY1160 using an antibody specific for the Hmg1p isozyme (against the 15 C-terminal amino acids). (C and D) Localization of Kar2p throughout the entire ER is shown for comparison in the same strain. (E and F) Increased levels of Hmg1p localized in strain JRY1239, which contains a multicopy *HMG1* plasmid. (G and H) Localization of Kar2p in strain JRY1239 is shown for comparison. Bar, 5 μm.

was even more challenging than Hmg1p to localize at endogenous levels. However, because *HMG2* mRNA and enzyme activity levels increase threefold under low oxygen or heme-depleted conditions (Thorsness *et al.*, 1989), we decided to use semi-anaerobic growth conditions to increase the levels of Hmg2p. In cells deleted for *HMG1* and grown semi-anaerobically, Hmg2p was localized in the nuclear envelope in a pattern similar to that of Hmg1p (Figure 8, A and B). Endogenous levels of Hmg2p were also localized in the nuclear envelope in cells grown aerobically, but the signal was very dim and the background staining high (our unpublished results). Finally, Hmg2p was similarly localized in the nuclear envelope in a semi-anaerobically grown strain containing both isozymes (our unpublished results). Kar2p immunofluorescence of the same strain is shown for comparison (Figure 8, C and D).

In cells with a multicopy *HMG2* plasmid, a different pattern of staining was detected in which bright patches and circular patterns of staining were evident around the periphery of the cells and on some nuclei (Figure 8, E and F). These patterns most likely represented strips, short karmellae, and whorls seen by electron microscopy. Faint staining of the nuclear envelope was also detectable in many cells. Like Hmg1p, Hmg2p was not distributed equally among all the cells. This variation may be due, in part, to differences in the copy number of the plasmid between cells. These observations indicate that Hmg2p is preferentially localized to the peripheral ER when overexpressed. Localization of Kar2p is shown for comparison (Figure 8, G and H).

Hmg2p Was Localized in the Membrane Proliferations by Immunoelectron Microscopy

Cells with elevated levels of Hmg2p were analyzed by immunoelectron microscopy to determine Hmg2p distribution. In these cells, an antiserum specific for Hmg2p labeled ER membrane proliferations: strips, whorls, and short karmellae (Figure 9, A and B). Occasionally, labeling was seen in the whorl interiors (our unpublished observations). However, labeling

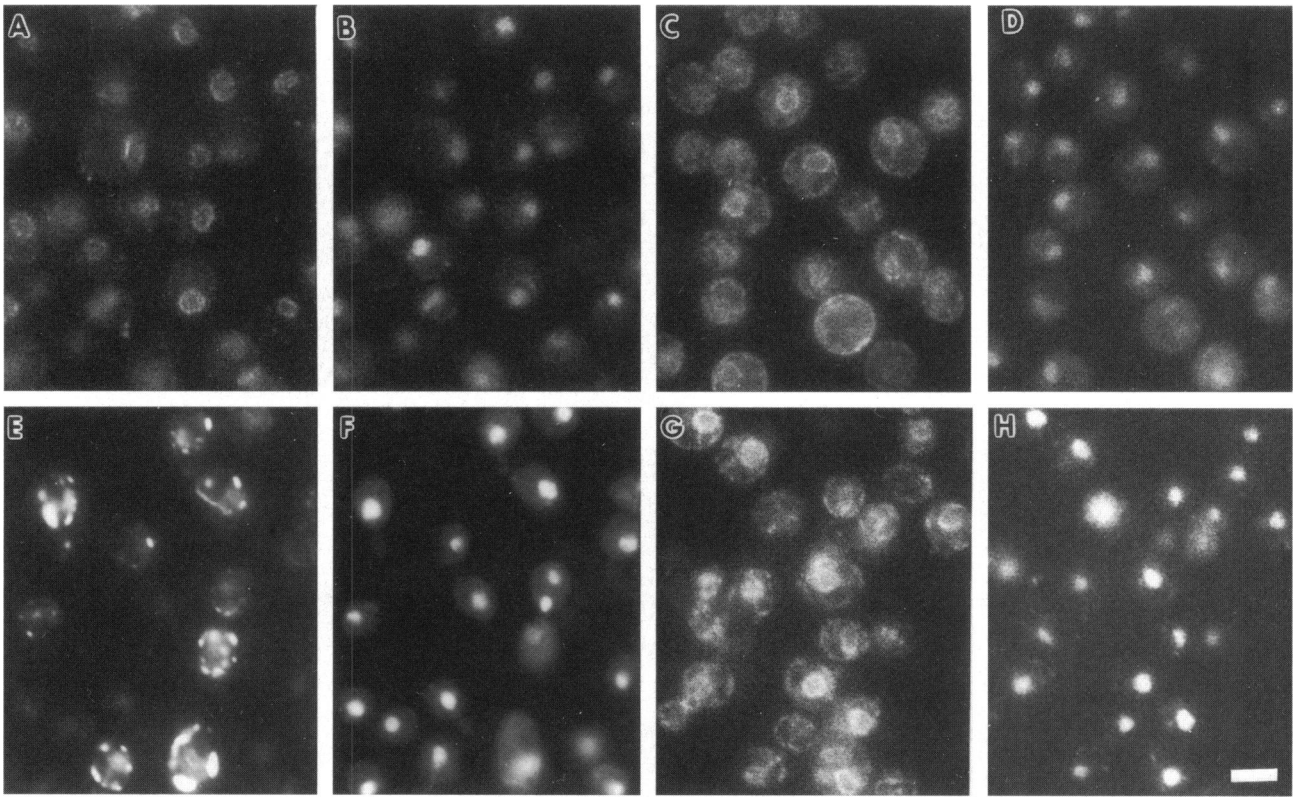

Figure 8. Localization of endogenous and increased levels of Hmg2p by indirect immunofluorescence. Indirect immunofluorescent localization of Hmg2p or Kar2p is shown in panels A, C, E, and G. Localization of the nucleus in the same cells is shown by DAPI staining in panels B, D, F, and H. (A and B) Localization of endogenous levels of Hmg2p was determined in cells of strain JRY1159 using an antibody specific for the Hmg2p isozyme (against the 15 C-terminal amino acids). These cells were grown semi-anaerobically to be able to detect Hmg2p. (C and D) Localization of Kar2p throughout the entire ER is shown for comparison in the same strain also in cells grown semi-anaerobically. (E and F) Increased levels of Hmg2p were localized in strain RWY306 (grown aerobically), which contains a multicopy *HMG2* plasmid. (G and H) Localization of Kar2p in strain RWY306 is shown for comparison. Bar, 5 μm.

density was very low in areas of the nuclear envelope and peripheral ER that had not proliferated. No significant immunolabeling of these membrane proliferations was detected with pre-immune serum (Figure 9C). These results were consistent with the Hmg2p localization pattern seen with indirect immunofluorescence.

Increased Levels of Hmg1 and Hmg2 GFP Fusions Colocalize Similarly with Sec61p but not with Kar2p

Colocalization studies of HMGR isozymes and other yeast ER proteins were performed to confirm that the membranes proliferated in response to these isozymes were derived from the ER. To facilitate this analysis, fusions of Hmg1p and Hmg2p to the *Aequorea* GFP (Prasher *et al.*, 1992) were constructed. To eliminate differences in transcription rates from the *HMG1* versus *HMG2* promoter, the GFP fusions were expressed under control of the inducible *GAL1* promoter. The patterns of fluorescence seen with Hmg1:GFP and Hmg2:GFP fusions were identical to the patterns of elevated levels of the native isozymes (compare Figure 7, E and F, and Figure 8, E and F, with Figure 10, GFP column). The bright GFP fluorescent areas represented membrane proliferations because these areas also stained with the ER membrane dye R6 (rhodamine B, hexyl ester chloride) in a pattern identical to that seen in Figures 1 and 2 (our unpublished observations). The staining properties of R6 are identical to that of DiOC6, except that R6 fluoresces red (Terasaki *et al.*, 1984). In addition, electron microscopy confirmed that karmellae membranes were induced by increased levels of the Hmg1:GFP fusion (Profant, Roberts, and Wright, unpublished observations). A similar Hmg2:GFP fusion has been previously reported (Hampton *et al.*, 1996), which was shown to be present in membrane proliferations stained with R6 and to induce Hmg2p-type membrane proliferations as seen by electron microscopy.

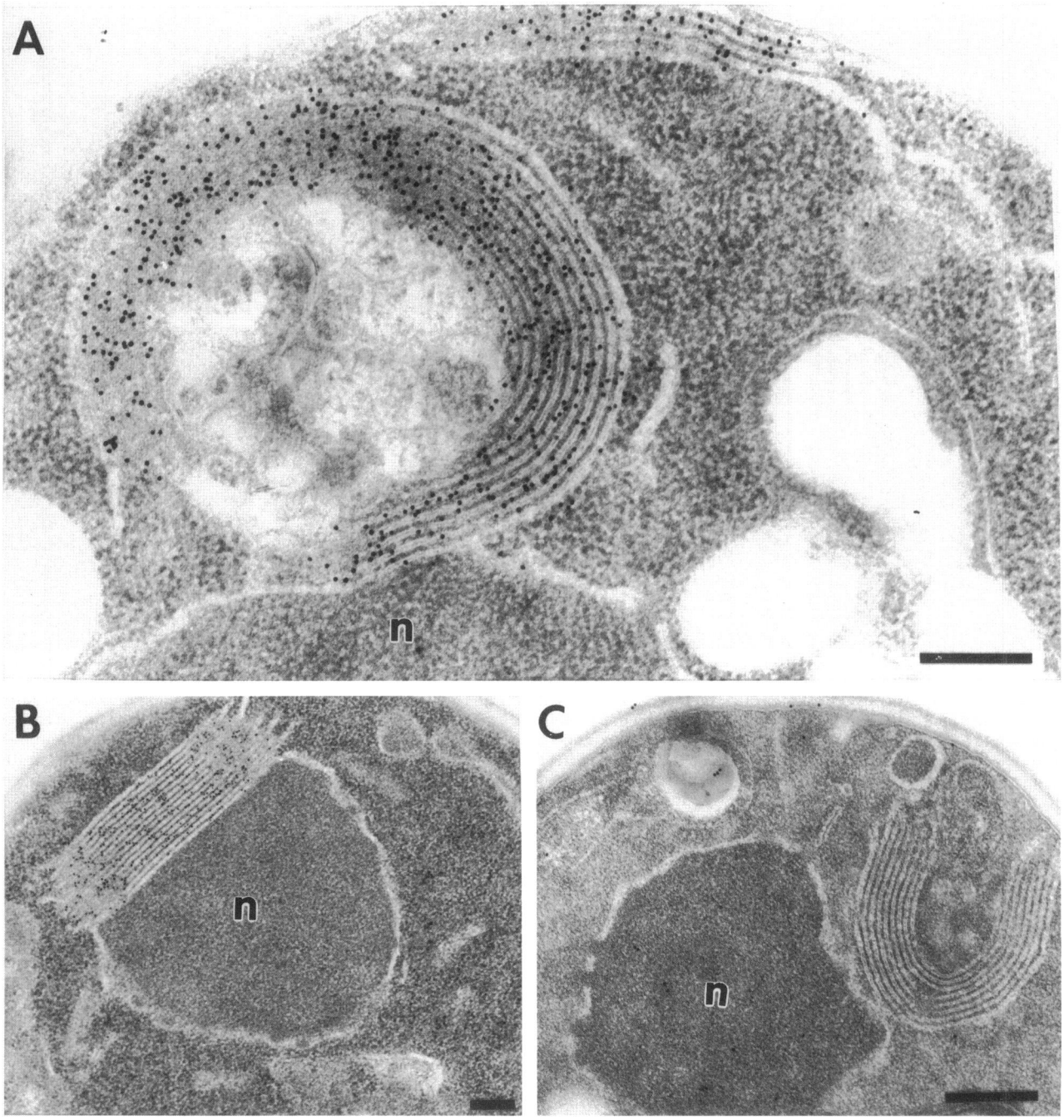

Figure 9. Localization of Hmg2p in strips, whorls, and short karmellae by immunoelectron microscopy. Cells of strain RWY446, which had high levels of Hmg2p, were immunolabeled as described in MATERIALS AND METHODS. (A) A whorl and peripheral strip of ER were densely labeled with gold particles; nucleus (n). (B) Short karmellae proliferation also contained high amounts of Hmg2p. (C) RWY446 cells treated with pre-immune serum. Bar, 200 nm.

Indirect immunofluorescence of Kar2p, a lumenal ER protein, and Sec61p, an integral ER membrane protein that is part of the translocation pore complex (see review by High and Stirling, 1993) were compared with the localization patterns of the Hmg1:GFP and Hmg2:GFP fusions. As a control for the procedure, both GFP fusions were colocalized successfully with an antibody that cross-reacts with both HMGR catalytic domains (Figure 10, row 3 [96% co-localization] and row 6 [98% colocalization]). Sec61p was

present in 89% of the membranes containing Hmg2:GFP (Figure 10, row 1), and 76% of the membranes containing Hmg1:GFP (Figure 10, row 4). Unexpectedly, Kar2p was present only 5% of the time in Hmg2:GFP-induced membranes (Figure 10, row 2), but in 74% of the membranes containing Hmg1:GFP (Figure 10, row 5). Therefore, both Hmg1:GFP and Hmg2:GFP colocalized similarly with the ER membrane protein Sec61p. However, the ER lumenal protein Kar2p was strikingly less abundant in the Hmg2:GFP-containing membrane proliferations than in the Hmg1:GFP-containing membrane proliferations.

Exchanging a Lumenal Loop of Hmg2p with the Corresponding Loop from the Membrane Domain of Hmg1p Altered the Distribution of Hmg2p

Recently, exchanges between regions of the Hmg1p membrane domain and Hmg2p membrane domain identified a region of the Hmg1p membrane domain that is responsible for the proliferation of karmellae (Parrish *et al.*, 1995). The 77-amino acid region of the protein between the last two membrane spanning regions, called Loop G (Figure 11E), was identified as necessary and sufficient to cause an Hmg2p construct containing Loop G from Hmg1p to produce karmellae. We have examined the subcellular localization of increased levels of this exchange construct compared with increased levels of native Hmg2p using indirect immunofluorescence. Instead of the mainly peripheral ER pattern distinctive of increased Hmg2p (Figure 11, A and B), the Hmg2p construct containing Loop G of Hmg1p was concentrated in the nuclear envelope in a pattern that appeared identical to that of increased levels of Hmg1p (Figure 11, C and D). Examination of the reciprocal exchange will be necessary to determine the role of the Hmg2p Loop G sequences in Hmg2p localization at increased expression levels.

DISCUSSION

Hmg1p- and Hmg2p-induced Membranes

Mammalian cells that synthesize abundant steroids produce smooth ER membrane proliferations, and presumably have naturally elevated levels of HMGR (Sisson and Fahrenbach, 1967; Black, 1972; Fringes and Gorgas, 1993). In addition, proliferation of membranes can be induced by artificially elevating HMGR levels with competitive inhibitors of HMGR, such as compactin (Chin *et al.*, 1982) and lovastatin (Singer *et al.*, 1988). Because elevated levels of serum cholesterol are important risk factors for developing heart disease, HMGR inhibitors are increasingly prescribed to reduce serum cholesterol levels. As a result, more than a million people are currently taking these drugs. Although we have not identified conditions under which yeast cells naturally produce elevated levels of HMGR sufficient to induce membrane proliferations, we have identified a yeast model in which we can investigate HMGR-induced membrane biogenesis. These studies may in turn lead to a better understanding of cellular membrane homeostasis, including that induced by HMGR inhibitors.

Despite some similarities, the membranes induced by Hmg1p and Hmg2p were morphologically and temporally distinct, and reflected the different localization patterns of the two isozymes when expressed at increased levels. Karmellae were the most abundant type of membrane proliferation induced by increased levels of Hmg1p except in late stages of growth when whorls became abundant. In contrast, the proportion of Hmg2p-expressing cells with short karmellae steadily decreased relative to the proportion of cells with strips and whorls as culture growth progressed. Since Hmg2p has a much shorter half-life than Hmg1p, the greater proportion of whorls in Hmg2p cultures may reflect the faster turnover of both Hmg2p and of Hmg2p-induced membranes. Indeed, stabilizing Hmg2p with lovastatin led to the persistence of Hmg2p-induced membrane proliferations long after they had disappeared in a parallel unstabilized culture. In *Schizosaccharomyces pombe*, whorls are thought to be intermediates in the degradation of HMGR-induced membranes (Lum and Wright, 1995). Our preliminary results suggest that whorls may be degradative intermediates in *S. cerevisiae* as well (our unpublished results).

It is interesting to note that both types of HMGR-induced karmellae preferentially arose from the nuclear envelope on the side that contained the nucleolus. This asymmetry reflected the natural polarity of the yeast nucleus in which the spindle pole body is positioned opposite the nucleolus (Yang *et al.*, 1989). The asymmetry of these karmellae membranes is not attributable to the budding pattern of *S. cerevisiae* division, because karmellae are also preferentially found on the nucleolar side of the nucleus in fission yeast (Lum and Wright, unpublished results). These results suggest that elevated levels of HMGR may reveal additional specialized regions that exist within the nuclear envelope.

Localization of Hmg1p and Hmg2p

Due to the density of ribosomes in the yeast cytoplasm, identifying even classical ER subdomains such as smooth and rough ER is difficult. However, a clear distinction can be made in yeast between the nuclear envelope and the remainder of the ER. For example, components of the nuclear pores localize predominantly in the nuclear envelope (Aitchison *et al.*, 1995; Li *et al.*, 1995; Strambio-de-Castillia *et al.*, 1995). Many other yeast ER proteins show no apparent enrichment in specialized subdomains, but are instead found

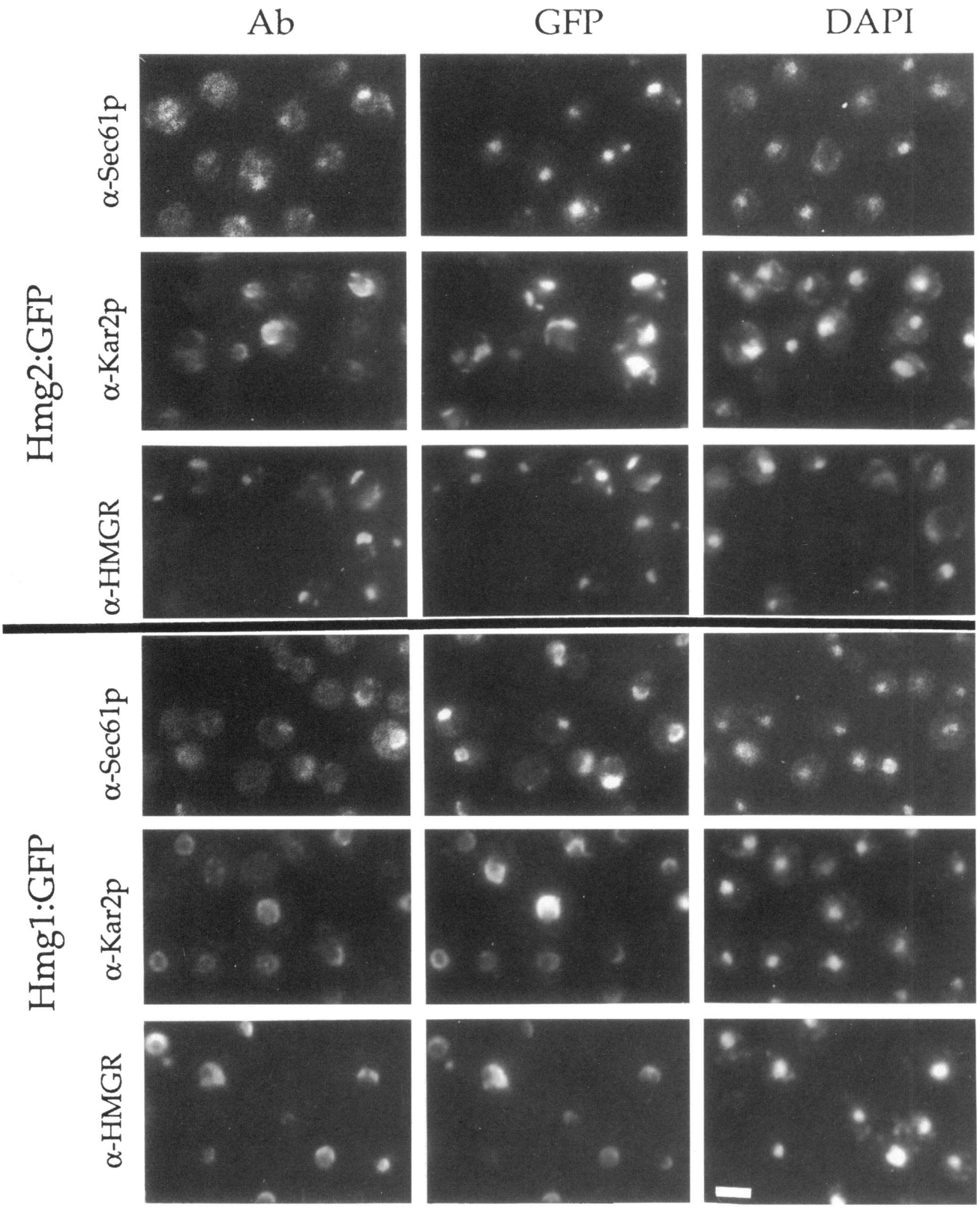
Ab
GFP
DAPI
Hmg2:GFP
α-Sec61p
α-Kar2p
α-HMGR
Hmg1:GFP
α-Sec61p
α-Kar2p
α-HMGR

Figure 10.

throughout the ER (Rose *et al.*, 1989; Feldheim *et al.*, 1992; Hill and Stevens, 1994; Schlenstedt *et al.*, 1995). A possible exception is Cne1p, a calnexin homologue, which appears to be enriched in the nuclear envelope in a pattern similar to that of Hmg1p at increased levels (Figure 8D in Parlati *et al.*, 1995). Thus, specialization within the yeast ER has not been readily apparent for proteins other than nucleoporins and spindle-pole body components. However, to the limits of our detection, endogenous levels of Hmg1p and Hmg2p were both predominantly localized in an ER subdomain: the nuclear envelope.

Interestingly, with a moderate 10- to 16-fold increase in the amount of HMGR, the two yeast HMGR isozymes showed different localization patterns. Hmg1p was still localized predominantly in the nuclear envelope, whereas Hmg2p was found predominantly in the peripheral ER. In contrast, many other yeast ER proteins are not preferentially localized in different ER subdomains when overexpressed (Deshaies and Schekman, 1990; Preuss *et al.*, 1991; Tachibana and Stevens, 1992; Esnault *et al.*, 1993; Chapman and Munro, 1994; Hamburger *et al.*, 1995). Thus, the localization of increased levels of Hmg1p and Hmg2p in different regions of the ER is not a general feature of the yeast ER proteins studied so far. Moreover, increased levels of both Hmg1:GFP and Hmg2:GFP colocalized with Sec61p, demonstrating that these membrane proliferations were derived from the ER. In contrast, although Kar2p (BiP) did colocalize with Hmg1:GFP, Kar2p did not colocalize appreciably with Hmg2:GFP. This result was unexpected because Kar2p is involved in the translocation of proteins into the ER, and therefore its distribution would be expected to be similar to that of Sec61p, a component of the translocation pore. Recently, the distribution of Kar2p in the yeast ER was examined with IEM (Bachem and Mendgen, 1995). In these studies, Kar2p was least abundant in the nuclear envelope, more abundant in the cortical ER (near the cell periphery), and most abundant in the internal ER (excluding the nuclear envelope and cortical ER). Since it is thought that BiP can diffuse freely within the ER (Ceriotti and Colman, 1988), Kar2p may have restricted access to the Hmg2p-induced membranes, because it was not localized appreciably in either the nuclear or peripherally located membrane proliferations induced by Hmg2p.

An interesting difference between Hmg2p and Hmg1p is that the localization of Hmg2p was altered when the protein was expressed at high versus low levels. Since endogenous levels of Hmg2p were difficult to detect by immunofluorescence, it may be that the techniques used were not sensitive enough to observe Hmg2p in the peripheral ER. However, even if the two isozymes have similar distributions at endogenous levels of expression, each protein may organize a different microdomain in the nuclear envelope that contains different sets of associated proteins. Thus, the two proteins might appear to be uniformly localized throughout the nuclear envelope, but actually be present in nonoverlapping, interspersed microdomains. The distinct patterns of membrane proliferations induced by Hmg1p versus Hmg2p would then reflect the consequences of expansion of these different microdomains.

We may gain insight into the differences between the two isozymes by investigating regions of the two proteins that are required for their different localization patterns at increased expression levels. Increased levels of Hmg2p containing Loop G from Hmg1p displayed the localization pattern of Hmg1p. This result suggested that the Loop G of Hmg1p contained a signal that retained the majority of Hmg1p in the nuclear envelope. Alternatively, information necessary to localize increased levels of Hmg2p to the peripheral ER may have been lost, resulting in a localization resembling that of Hmg1p. Our preliminary results in localizing a chimeric version of Hmg1p that contains Loop G sequences from Hmg2p support the second possibility. When expressed at increased levels, a chimeric Hmg1p with Loop G from Hmg2p was localized to the nuclear envelope in a pattern resembling increased levels of native Hmg1p (our unpublished results). Therefore, Loop G sequences from Hmg2p were necessary for its localization pattern at increased levels of expression, but not sufficient to confer Hmg2p localization when expressed in the context of native Hmg1p. Further experiments are underway to investigate the role of Loop G and other regions of the protein in the localization of Hmg1p and Hmg2p.

(Figure 10 cont.) Colocalization of Hmg1:GFP and Hmg2:GFP with other ER proteins. Cells containing the galactose-inducible GFP fusions of Hmg1p (RWY621) or Hmg2p (RWY663) were grown in galactose/raffinose medium to induce the expression of the proteins, and then fixed and prepared for indirect immunofluorescence. The left column labeled "Ab" shows the immunofluorescent pattern of different antibody treatments. The center column labeled "GFP" shows the fluorescence of the GFP fusions in the same cells. And the right column labeled "DAPI" shows the location of the nuclei in the same cells. Rows 1-3 contain cells expressing the Hmg2p:GFP fusion. (Row 1) Sec61p colocalized with Hmg2:GFP. (Row 2) Kar2p did not colocalize extensively with Hmg2:GFP. (Row 3) Hmg2:GFP was recognized by antibodies against the conserved catalytic domain of Hmg1p demonstrating that the procedure was effective. Rows 4-6 contain cells expressing the Hmg1:GFP fusion. (Row 4) Sec61p colocalized with Hmg1:GFP. (Row 5) Kar2p colocalized with Hmg1:GFP. (Row 6) Hmg1:GFP was recognized with an antibody against the catalytic domain. No bleedthrough of GFP fluorescence was seen in the red channel in controls lacking treatment with primary antibody. Bar, 5 μm.

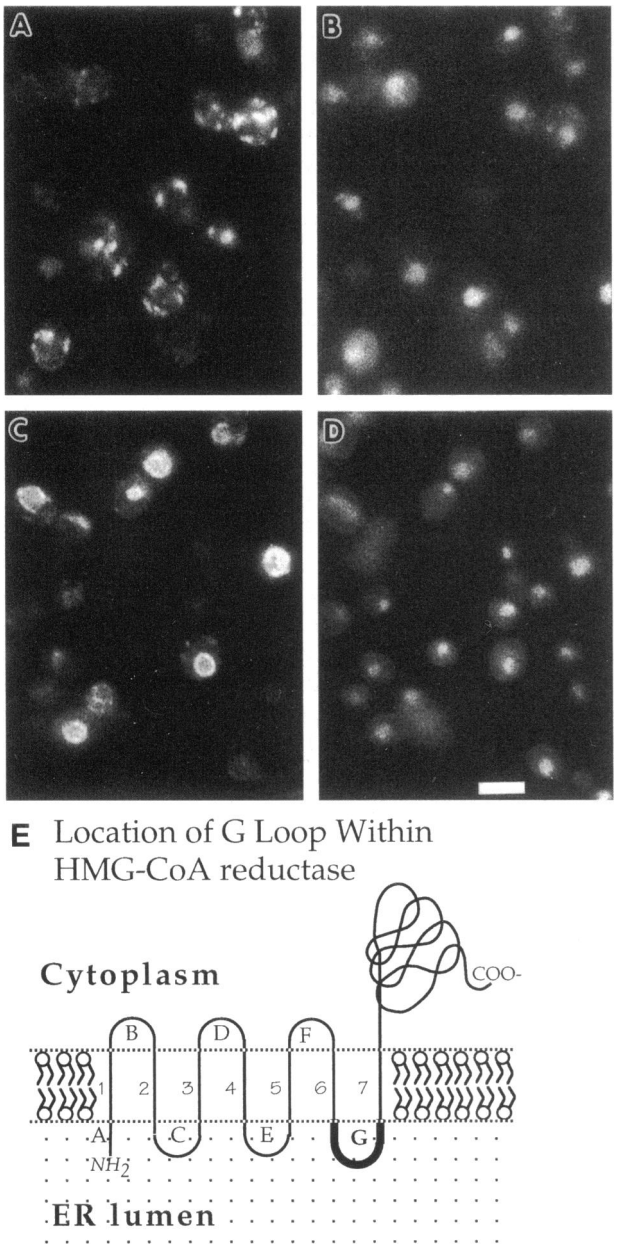

Figure 11. Substituting the Loop G of Hmg2p with that of Hmg1p alters the Hmg2p distribution in the ER. (A and B) Immunofluorescent localization of increased levels of Hmg2p (RWY605), and localization of the nucleus in the same cells by DAPI staining. (C and D) Immunofluorescent localization of cells containing increased levels of the Hmg2p construct containing Loop G of Hmg1p (RWY590), and localization of the nucleus in the same cells by DAPI staining. In both cases an antiserum against the C-terminal 15 amino acids of Hmg2p was used to detect the proteins. (E) Loop G is predicted to lie in the ER lumen between the last two membrane spanning regions of HMG-CoA reductase.

Why Two Isozymes of HMGR?

All animals appear to require only a single HMGR isozyme. Why then does the simpler, unicellular fungus *S. cerevisiae* encode two isozymes of HMGR? Part of the answer may lie in the differential expression of the HMGR genes in response to oxygen levels and to heme (whose levels reflect oxygen availability). The differential expression of *HMG1* versus *HMG2* under different oxygen levels acts as a buffer so that changing levels of heme do not affect the total levels of HMGR in the cell (Thorsness *et al.*, 1989). Similar to *HMG1* and *HMG2*, subunit V of the yeast mitochondrial cytochrome c oxidase complex and cytochrome c are encoded by different isoforms whose abundance changes depending on the cellular levels of heme (Guarente and Mason, 1983; Laz *et al.*, 1984; Trueblood *et al.*, 1988). It has been suggested that the more abundant subunits under low oxygen conditions are better adapted to those conditions and possibly to interactions with each other (Trueblood *et al.*, 1988). Likewise, Hmg1p may be better suited for aerobic conditions and Hmg2p for low oxygen conditions. For example, under heme-depleted conditions, the specific activity of HMGR in cells expressing only Hmg2p is 10-fold higher than in cells expressing only Hmg1p, yet the cells with the Hmg2p isozyme produce 24-fold more sterols (Casey *et al.*, 1992). This result suggests that under heme-depleted conditions the pathway containing the Hmg2p isozyme is better adapted to synthesize sterols than the pathway containing Hmg1p. Since yeast cells are likely to encounter variable oxygen conditions in their natural environment, the ability to buffer both the levels and isoforms of HMGR may be important for cell viability. Indeed, in a competition experiment under normal laboratory culture conditions, cells with both forms of HMGR out-competed cells with only one or the other isozyme (Basson *et al.*, 1987).

Another indication that the presence of two HMGR isozymes is important to the cell follows from research on the fate of mevalonate, the product of the reaction catalyzed by both Hmg1p and Hmg2p (Casey *et al.*, 1992). Since mevalonate is soluble, it might be expected to have the same fate regardless of which HMGR isozyme produced it. However, results from Casey and colleagues suggest that the mevalonate produced by the two HMGR isozymes is not equally available to all elements of the mevalonate pathway (Casey *et al.*, 1992). Specifically, they report that the production of sterols from Hmg1p-derived mevalonate is limited by palmitoleic acid availability, unaffected by oleic acid, and strongly inhibited by ergosterol (the yeast equivalent of cholesterol). In contrast, the production of sterols from Hmg2p-derived mevalonate is unaffected by palmitoleic acid, decreased by oleic acid, and slightly decreased by ergosterol. Surprisingly, these effects were not due to altered expression or activity of the HMGR isozymes, but instead, reflected the isozyme-specific source of the mevalonate. This result led the authors to suggest that the

two isozymes are physiologically compartmentalized (Casey *et al.*, 1992). Consistent with this possibility, our results suggested that, at least at elevated levels, Hmg1p and Hmg2p were physically compartmentalized, being concentrated preferentially in different regions of the ER.

By analyzing different responses of yeast to increased levels of the HMGR isozymes we have uncovered differences that are undetectable at endogenous levels of expression. Such differences included induction of distinct sets of membrane proliferations with different protein compositions and the presence of a lumenal region of Hmg2p that was necessary for its localization pattern when expressed at increased levels. Together with the results that suggest isozyme-specific fates of mevalonate in the sterol pathway (Casey *et al.*, 1992), the evidence suggests that HMGR isozymes interact with different sets of cellular proteins. Thus, the particular regions of the ER proliferated in response to elevated HMGR levels may reveal ER regions specialized for specific branches of the sterol biosynthetic pathway that are undetectable at endogenous expression levels of HMGR.

ACKNOWLEDGMENTS

We thank the members of the Wright Lab for their helpful advice, discussions, and support. In addition, we thank Randy Hampton for providing the Gal *HMG2* construct (pRH134-2), Mark Rose for providing the Kar2p antiserum, Jeff Brodsky for providing the Sec61p antiserum, and Jeff Cox and Peter Walter for providing the GFP construct. This research was supported by a pre-doctoral National Science Foundation Fellowship and National Institutes of Health Molecular and Cellular Biology Training Grant 5T32GM-07270-27 (A.K.) and grant GM-45726 (C.R. and R.W.).

REFERENCES

Aitchison, J.D., Blobel, G., and Rout, M.P. (1995). Nup120p: a yeast nucleoporin required for NPC distribution and mRNA transport. J. Cell Biol. *131*, 1659-1675.

Bachem, U., and Mendgen, K. (1995). Endoplasmic reticulum subcompartments in a plant parasitic fungus and in baker's yeast: differential distribution of lumenal proteins. Exp. Mycol. *19*, 137-152.

Basson, M.E., Moore, R.L., O'Rear, J., and Rine, J. (1987). Identifying mutations in duplicated functions in *Saccharomyces cerevisiae*: recessive mutations in HMG-CoA reductase genes. Genetics *117*, 645-655.

Basson, M.E., Thorsness, M.K., Finer-Moore, J., Stroud, R., and Rine, J. (1988). Structural and functional conservation between yeast and human 3-hydroxy-3-methylglutaryl coenzyme A reductases, the rate-limiting enzyme of sterol biosynthesis. Mol. Cell. Biol. *9*, 3797-3808.

Basson, M.L., Thorsness, M.K., and Rine, J. (1986). *Saccharomyces cerevisiae* contains two functional genes encoding 3-hydroxy-3-methylglutaryl coenzyme A reductase. Proc. Natl. Acad. Sci. USA *83*, 5563-5567.

Black, V.H. (1972). The development of smooth-surfaced endoplasmic reticulum in adrenal cortical cells of fetal guinea pigs. Am. J. Anat. *156*, 318-418.

Byers, B., and Goetsch, L. (1991). Preparation of yeast cells for thin-section electron microscopy. Methods Enzymol. *194*, 602-608.

Casey, W.M., Keesler, G.A., and Parks, L.W. (1992). Regulation of partitioned sterol biosynthesis in *Saccharomyces cerevisiae*. J. Bacteriol. *174*, 7283-7288.

Ceriotti, A., and Colman, A. (1988). Binding to membrane proteins within the endoplasmic reticulum cannot explain the retention of the glucose-regulated protein GRP78 in *Xenopus* oocytes. EMBO J. *7*, 622-638.

Chalfie, M., Tu, Y., Euskirchen, G., Ward, W.W., and Prasher, D.C. (1994). Green fluorescent protein as a marker for gene expression. Science *263*, 802-805.

Chapman, R.E., and Munro, S. (1994). The functioning of the yeast Golgi apparatus requires an ER protein encoded by ANP1, a member of a new family of genes affecting the secretory pathway. EMBO J. *13*, 4896-4907.

Chin, D.J., Luskey, K.L., Anderson, R.G.W., Faust, J.R., Goldstein, J.L., and Brown, M.S. (1982). Appearance of crystalloid endoplasmic reticulum in compactin-resistant Chinese hamster cells with a 500-fold elevation in 3-hydroxy-3-methylglutaryl coenzyme A reductase. Proc. Natl. Acad. Sci. USA *79*, 1185-1189.

Deschenes, R.J., and Broach, J.R. (1987). Fatty acylation is important but not essential for *Saccharomyces cerevisiae RAS* function. Mol. Cell Biol. *7*, 2344-2351.

Deshaies, R.J., and Schekman, R. (1990). Structural and functional dissection of Sec62p, a membrane-bound component of the yeast endoplasmic reticulum protein import machinery. Mol. Cell Biol. *10*, 6024-6035.

Esnault, Y., Blondel, M.-O., Deshaies, R.J., Schekman, R., and Kepes, F. (1993). The yeast SSS1 gene is essential for secretory protein translocation and encodes a conserved protein of the endoplasmic reticulum. EMBO J. *12*, 4083-4093.

Fawcett, D.W. (1981). The Cell, 2nd ed., Philadelphia, PA: W.B. Saunders, 301-368.

Feldheim, D., Rothblatt, J., and Schekman, R. (1992). Topology and functional domains of Sec63p, an endoplasmic reticulum membrane protein required for secretory protein translocation. Mol. Cell Biol. *12*, 3288-3296.

Franzini-Armstrong, C., Kenney, L.J., and Varriano-Marston, E. (1987). The structure of calsequestrin in triads of vertebrate skeletal muscle: a deep-etch study. J. Cell Biol. *105*, 49-56.

Fringes, B., and Gorgas, K. (1993). Crystalloid smooth endoplasmic reticulum in the quail uropygial gland. Ann. Anat. *175*, 231-235.

Gaigg, B., Simbeni, R., Hrastnik, C., Paltauf, F., and Daum, G. (1995). Characterization of a microsomal subfraction associated with mitochondria of the yeast, *Saccharomyces cerevisiae*: involvement in synthesis and import of phospholipids into mitochondria. Biochim. Biophys. Acta *1234*, 214-220.

Galteau, M.M., Antoine, B., and Reggio, H. (1985). Epoxide hydrolase is a marker for the smooth endoplasmic reticulum in rat liver. EMBO J. *4*, 2793-2800.

Gil, G., Faust, J.R., Chin, D.J., Goldstein, J.L., and Brown, M.S. (1985). Membrane-bound domain of HMG-CoA reductase is required for sterol-enhanced degradation of the enzyme. Cell *41*, 249-258.

Goldstein, J.L., and Brown, M.S. (1990). Regulation of the mevalonate pathway. Nature *343*, 425-430.

Guarente, L., and Mason, T. (1983). Heme regulates the transcription of the *CYC1* gene of *S. cerevisiae* via an upstream activation site. Cell *32*, 1279-1286.

Hamburger, D., Egerton, M., and Riezman, H. (1995). Yeast Gaa1p is required for attachment of a completed GPI anchor onto proteins. J. Cell Biol. *129*, 629-639.

Hampton, R.Y., Koning, A., Wright, R., and Rine, J. (1996). In vivo examination of membrane protein localization and degradation with GFP. Proc. Natl. Acad. Sci. USA *93*, 828–833.

Hampton, R.Y., and Rine, J. (1994). Regulated degradation of HMG-CoA reductase, an integral membrane protein of the endoplasmic reticulum, in yeast. J. Cell Biol. *125*, 299-312.

High, S., and Stirling, C.J. (1993). Protein translocation across membranes: common themes in divergent organisms. Trends Cell Biol. *3*, 335-339.

Hill, K.J., and Stevens, T.H. (1994). Vma21p is a yeast membrane protein retained in the endoplasmic reticulum by a di-lysine motif and is required for the assembly of the vacuolar H^+-ATPase complex. Mol. Biol. Cell *5*, 1039-1050.

Jingami, H., Brown, M.S., Goldstein, J.L., Anderson, R.G.W., and Luskey, K.L. (1987). Partial deletion of membrane-bound domain of 3-hydroxy-3-methylglutaryl coenzyme A reductase eliminates sterol-enhanced degradation and prevents formation of crystalloid endoplasmic reticulum. J. Cell. Biol. *104*, 1693-1704.

Koning, A.J., Lum, P.Y., Williams, J.M., and Wright, R. (1993). $DiOC_6$ staining reveals organelle structure and dynamics in living yeast cells. Cell Motil. Cytoskeleton *25*, 111-128.

Laz, T.M., Pietras, D.F., and Sherman, F. (1984). Differential regulation of the duplicated iso-cytochrome c genes in yeast. Proc. Natl. Acad. Sci. USA *81*, 4475-4479.

Li, O., Heath, C.V., Amberg, D.C., Dockendorff, T.C., Copeland, C.S., Snyder, M., and Cole, C.N. (1995). Mutation or deletion of the *Saccharomyces cerevisiae RAT3/NUP133* gene causes temperature-dependent nuclear accumulation of poly(A)+ RNA and constitutive clustering of nuclear pore complexes. Mol. Biol. Cell *6*, 410-417.

Lum, P.Y., and Wright, R. (1995). Degradation of HMG Co-A reductase-induced membranes in the fission yeast, *Schizosaccharomyces pombe*. J. Cell Biol. *131*, 81-94.

Maniatis, T., Fritsch, E.F., and Sambrook, J. (1982). Molecular Cloning: A Laboratory Manual, Cold Spring Harbor, NY: Cold Spring Harbor Laboratory Press.

Matile, P., Moor, H., and Robinow, C.F. (1969). The Yeasts. In: Yeast Cytology, vol. I, New York: Academic Press, 219-302.

Nishikawa, S., Hirata, A., and Nakano, A. (1994). Inhibition of endoplasmic reticulum (ER)-to-Golgi transport induces relocalization of binding protein (BiP) within the ER to form Bip bodies. Mol. Biol. Cell *5*, 1129-1143.

Palade, G.E. (1975). Intracellular aspects of the process of protein synthesis. Science *189*, 347-358.

Parlati, F., Dominguez, M., Bergeron, J.J., and Thomas, D.Y. (1995). *Saccharomyces cerevisiae CNE1* encodes an endoplasmic reticulum (ER) membrane protein with sequence similarity to calnexin and calreticulum and functions as a constituent of the ER quality control apparatus. J. Biol. Chem. *270*, 244-253.

Parrish, M., Sengstag, C., Rine, J., and Wright, R. (1995). Identification of the sequences in HMG-CoA reductase required for karmellae assembly. Mol. Biol. Cell *6*, 1535-1547.

Pathak, R.K., Luskey, K.L., and Anderson, R.G.W. (1986). Biogenesis of the crystalloid endoplasmic reticulum in UT-1 cells: evidence that newly formed endoplasmic reticulum emerges from the nuclear envelope. J. Cell Biol. *102*, 2158-2168.

Prasher, D.C., Eckenrode, V.K., Ward, W.W., Prendergast, F.G., and Cormier, M.J. (1992). Primary structure of the *Aequorea victoria* green-fluorescent protein. Gene *111*, 229-233.

Preuss, D., Mulholland, J., Kaiser, C.A., Orlean, P., Albright, C., Rose, M.D., Robbins, P.W., and Botstein, D. (1991). Structure of the yeast endoplasmic reticulum: localization of ER proteins using immunofluorescence and immunoelectron microscopy. Yeast *7*, 891-911.

Pringle, J.R., Preston, R.A., Adams, A.E.M., Stearns, T., Drubin, D.G., Haarer, B.K., and Jones, E.W. (1989). Fluorescence microscopy methods for yeast. Methods Cell Biol. *31*, 357-435.

Reynolds, E.S. (1963). The use of lead citrate at high pH as an electron-opaque stain in electron microscopy. J. Cell Biol. *17*, 208-212.

Roitelman, J., and Simoni, R.D. (1992). Distinct sterol and nonsterol signals for the regulated degradation of 3-hydroxy-3-methylglutaryl-CoA reductase. J. Biol. Chem. *267*, 25264-25273.

Rose, J.K., and Doms, R.W. (1988). Regulation of protein export from the endoplasmic reticulum. Annu. Rev. Cell Biol. *4*, 257-288.

Rose, M.D., and Broach, J.R. (1991). Cloning genes by complementation in yeast. Methods Enzymol. *194*, 195-230.

Rose, M.D., Mistra, L.M., and Vogel, J.P. (1989). KAR2, a karyogamy gene, is the yeast homolog of the mammalian BiP/GRP78 gene. Cell *57*, 1211-1221.

Satoh, T., Ross, C.A., Villa, A., Supattapone, S., Pozzan, T., Snyder, S.H., and Meldolesi, J. (1990). The inositol 1,4,5-trisphosphate receptor in cerebellar Purkinje cells: quantitative immunogold labeling reveals concentration in an endoplasmic reticulum subcompartment. J. Cell Biol. *111*, 615-624.

Schlenstedt, G., Harris, S., Risse, B., Lill, R., and Silver, P.A. (1995). A yeast DnaJ homologue, Scj1p, can function in the endoplasmic reticulum with BiP/Kar2p via a conserved domain that specifies interactions with Hsp70s. J. Cell Biol. *129*, 979-988.

Sengstag, C., Stirling, C., Schekman, R., and Rine, J. (1990). Genetic and biochemical evaluation of eukaryotic membrane protein topology: the polytopic structure of *S. cerevisiae* HMG-CoA reductase. Mol. Cell. Biol. *10*, 672-680.

Sikorski, R.S., and Hieter, P. (1989). A uniform set of multipurpose shuttle vectors and yeast host strains designed for efficient manipulation of DNA in *S. cerevisiae*. Genetics *122*, 19-27.

Singer, I.I., Scott, S., Kazizis, D.M., and Huff, J.W. (1988). Lovastatin, an inhibitor of cholesterol synthesis, induces hydroxymethylglutaryl-coenzyme A reductase directly on membranes of expanded smooth endoplasmic reticulum in rat hepatocytes. Proc. Natl. Acad. Sci. USA *85*, 5264-5268.

Sisson, J.K., and Fahrenbach, W.H. (1967). Fine structure of steroidogenic cells of a primate cutaneous organ. Am. J. Anat. *121*, 337-368.

Sitia, R., and Meldolesi, J. (1992). Endoplasmic reticulum: a dynamic patchwork of specialized subdomains. Mol. Biol. Cell *3*, 1067-1072.

Skalnik, D.G., Narita, H., Kent, C., and Simoni, R.D. (1988). The membrane domain of 3-hydroxy-3-methylglutaryl coenzyme A reductase confers endoplasmic reticulum localization and sterol-regulated degradation onto β-galactosidase. J. Biol. Chem. *263*, 6836-6841.

Smith, S., and Blobel, G. (1993). The first membrane spanning region of the lamin B receptor is sufficient for sorting to the inner nuclear membrane. J. Cell Biol. *120*, 631-637.

Strambio-de-Castillia, C., Blobel, G., and Rout, M.P. (1995). Isolation and characterization of nuclear envelopes from the yeast *Saccharomyces*. J. Cell Biol. *131*, 19-31.

Tachibana, C., and Stevens, T.H. (1992). The yeast EUG1 gene encodes an endoplasmic reticulum protein that is functionally related to protein disulfide isomerase. Mol. Cell. Biol. *12*, 4601-4611.

Takei, K., Stukenbrok, H., Metcalf, A., Mignery, G.A., Sudhof, T.C., Volpe, P., and Camilli, P.D. (1992). Ca^{2+} stores in Purkinje neurons: endoplasmic reticulum subcompartments demonstrated by the heterogeneous distribution of the $InsP_3$ receptor, Ca^{2+}-ATPase, and calsequestrin. J. Neurosci. *12*, 489-505.

Terasaki, M., Song, J., Wong, J.R., Weiss, M.J., and Chen, L.B. (1984). Localization of endoplasmic reticulum in living and glutaraldehyde-fixed cells with fluorescent dyes. Cell *38*, 101-108.

Thorsness, M., Schafer, W., D'Ari, L.A., and Rine, J. (1989). Positive and negative transcriptional control by heme of genes encoding HMG-CoA reductase in *Saccharomyces cerevisiae*. Mol. Cell. Biol. *9*, 5702-5712.

Trueblood, C.E., Wright, R.M., and Poyton, R.O. (1988). Differential regulation of the two genes encoding *Saccharomyces cerevisiae* cytochrome c oxidase subunit V by heme and the *HAP2* and *REO1* genes. Mol. Cell Biol. *8*, 4537-4540.

Vertel, B.M., Walters, L.M., and Mills, D. (1992). Subcompartments of the endoplasmic reticulum. Semin. Cell Biol. *3*, 325-341.

Villa, A., Podini, P., Clegg, D.O., Pozzan, T., and Meldolesi, J. (1991). Intracellular Ca^{2+} stores in Purkinje neurons: differential distribution of the low affinity-high capacity Ca^{2+} binding protein, calsequestrin, of Ca^{2+} ATPase and of the ER lumenal protein, Bip. J. Cell Biol. *113*, 779-791.

Wright, R., Basson, M., D'Ari, L., and Rine, J. (1988). Increased amounts of HMG-CoA reductase induce "karmellae": a proliferation of stacked membrane pairs surrounding the yeast nucleus. J. Cell Biol. *107*, 101-114.

Wright, R., Keller, G., Gould, S.J., Subramani, S., and Rine, J. (1990). Cell-type control of membrane biogenesis induced by HMG-CoA reductase overproduction. New Biol. *2*, 915-921.

Wright, R., and Rine, J. (1989). Transmission electron microscopy and immunocytochemical studies of yeast: analysis of HMG-CoA reductase overproduction by electron microscopy. Methods Cell Biol. *31*, 473-512.

Yang, C.H., Lambie, E.J., Hardin, J., Craft, J., and Snyder, M. (1989). Higher order structure is present in the yeast nucleus: autoantibody probes demonstrate that the nucleolus lies opposite the spindle pole body. Chromosoma *98*, 123-128.